Cumulative reaction probability and reaction eigenprobabilities from time-independent quantum scattering theory

Oleg I. Tolstikhin*
Russian Research Center ''Kurchatov Institute,'' Kurchatov Square 1, Moscow 123182, Russia

Valentin N. Ostrovsky
Institute of Physics, The University of St. Petersburg, St. Petersburg 198904, Russia

Hiroki Nakamura
Division of Theoretical Studies, Institute for Molecular Science, Myodaiji, Okazaki 444, Japan
(Received 27 September 2000; published 14 March 2001)

The cumulative reaction probability (CRP) is a gross characteristic of rearrangement collision processes defining the reaction rate constant. This paper presents a complete development of the approach to the theory of CRP that we have recently proposed [Phys. Rev. Lett. **80**, 41 (1998)]. In the core of this approach lies an alternative expression for CRP in terms of the outgoing wave Green's function which is formally equivalent to the Miller's definition of this quantity in terms of the scattering matrix [J. Chem. Phys. **62**, 1899 (1975)] and to the Miller-Schwartz-Tromp formula [J. Chem. Phys. **79**, 4889 (1983)], but is direct, in contrast to the former, and more suitable for practical calculations than the latter. Furthermore, our approach rests on solid grounds of time-independent quantum scattering theory and provides an appealing competitive alternative to the absorbing potential formulation given by Seideman and Miller [J. Chem. Phys. **96**, 4412 (1992); **97**, 2499 (1992)]. Ideologically, it is close to the approach considered earlier for a one-dimensional model by Manolopoulos and Light [Chem. Phys. Lett. **216**, 18 (1993)], but is formulated from scratch for realistic systems with many degrees of freedom. The strongest point of our approach is that its final working formulas are expressed in terms of the Wigner-Eisenbud $\mathcal{R}$ matrix, so they can be easily implemented on the basis of many existing quantum scattering codes. All these features are discussed and illustrated by calculations of the CRP and reaction eigenprobabilities for two prototypical light atom transfer reactions in heavy-light-heavy triatomic systems in three dimensions for zero total angular momentum.

DOI: 10.1103/PhysRevA.63.042707 PACS number(s): 34.10.+x, 34.50.Lf, 82.20.Pm

I. INTRODUCTION

In the time-independent quantum scattering theory, the results of collisions between atomic particles are described by the scattering matrix $\mathbf{S}(E)$ which is a function of the total energy E of the system. This matrix defines the probabilities of all possible state-to-state transitions, so the absolute majority of theoretical methods naturally aims at calculating $\mathbf{S}(E)$ or its particular elements. Meanwhile, such a detailed description is not always needed, and there are situations where the knowledge of some gross characteristic of the system with respect to a given type of processes would be sufficient. The less such a characteristic depends on the particular conditions of the collision experiment in which it could be measured, the more intrinsic property of the system it represents and the more meaningful it is from the theoretical viewpoint. Experimental conditions enter the theory via the asymptotic states of reactants and products with respect to which the scattering matrix $\mathbf{S}(E)$ is defined. So, the characteristic meant above should be expressible in terms of some invariants of the matrix $\mathbf{S}(E)$. One of such characteristics is the eigenphase shift sum defined by [1]

$$\exp[2i\delta(E)]=\det[\mathbf{S}(E)], \tag{1}$$

which provides a rough description of the spectrum of resonances. Note that $\delta(E)$ is completely independent of the choice of a specific set of the asymptotic states, because $\det[\mathbf{S}(E)]$ is invariant under any unitary transformation of this set. Another characteristic of this type, which is the focus of the present work, is the cumulative reaction probability (CRP). This quantity was introduced in scattering theory by Miller [2] and characterizes the gross efficiency of rearrangement processes. Let us assume, for simplicity, that there are only two arrangements, which we denote by a and b. In this case, the scattering matrix can be partitioned into four blocks,

$$\mathbf{S}(E)=\begin{pmatrix}\mathbf{S}_{aa}(E) & \mathbf{S}_{ab}(E)\\ \mathbf{S}_{ba}(E) & \mathbf{S}_{bb}(E)\end{pmatrix}, \tag{2}$$

with $\mathbf{S}_{ba}(E)=\mathbf{S}_{ab}^{T}(E)$, where T stands for transpose. Then the CRP for reactions between a and b is defined by

$$N_{ab}(E)=\sum_{n_a,n_b}^{\text{open}}|S_{n_a n_b}(E)|^2=\mathrm{tr}[\mathbf{S}_{ab}(E)\mathbf{S}_{ab}^{\dagger}(E)], \tag{3}$$

where $S_{n_a n_b}(E)$ are the elements of $\mathbf{S}_{ab}(E)$, n_a and n_b label different asymptotic states in the arrangements a and b, respectively, and summation runs over all the open channels. It

*Email address: oleg@muon.imp.kiae.ru

 ©2001 The American Physical Society

can be easily seen that $N_{ab}(E)$ is invariant under any unitary transformation mixing the asymptotic states *separately* in each arrangement.

Formula (3) expresses $N_{ab}(E)$ in terms of the elements of the reaction block $\mathbf{S}_{ab}(E)$ of scattering matrix (2), thus providing a recipe to calculate the CRP by the methods of scattering theory. However, it was early recognized that methods that would enable one to evaluate $N_{ab}(E)$ *directly*, i.e., without relying on the calculation of $\mathbf{S}_{ab}(E)$, are desirable and worth developing. There are two basic reasons for that. First, the knowledge of $N_{ab}(E)$ permits one to calculate the reaction rate constant [2], which in chemical applications is often the only characteristic required. Second, one can expect that $N_{ab}(E)$ is determined by a much smaller region of configuration space than that which is essential for calculating $\mathbf{S}_{ab}(E)$, this expectation being supported by successes of the transition state theory. Thus concentrating on $N_{ab}(E)$ rather than on $\mathbf{S}_{ab}(E)$ may enable one (i) to avoid calculations of unnecessary information and (ii) to reduce the computational labor. These two principal objectives have motivated the development of the theory of CRP.

The first formula that has opened a way for direct calculations of the CRP was obtained by Miller, Schwartz, and Tromp (MST) [3]:

$$N_{ab}(E)=2\pi^2\ \mathrm{tr}[F\delta(H-E)F\delta(H-E)]. \tag{4}$$

Here F is a properly defined flux operator and H is the Hamiltonian of the system. Despite the fact that Eq. (4) does not contain time explicitly, it was derived by starting from a time-dependent formulation and following a logical route similar (though not identical) to that used earlier by Yamamoto [4], based on the Kubo's theory of linear response [5]. More recently, Moiseyev [6] derived the MST formula (4) from the time-independent scattering theory, thus establishing the relation of this important result to the discipline where it actually belongs. The approach initiated in Refs. [3,4] turned out to be very fruitful and is currently widely used for direct calculations of reaction rate constants by time-dependent methods [7–9]. However, because of the difficulties in implementation, the MST formula (4) did not find much application within the time-independent framework, which prompted the search for a more suitable expression.

An alternative representation for $N_{ab}(E)$ was proposed by Seideman and Miller [10,11]:

$$N_{ab}(E)=4\ \mathrm{tr}[\varepsilon_a G_\varepsilon(E)\varepsilon_b G_\varepsilon^*(E)], \tag{5}$$

where the operator $G_\varepsilon(E)$ is defined by

$$G_\varepsilon(E)=(H-E-i\varepsilon)^{-1},\quad \varepsilon=\varepsilon_a+\varepsilon_b. \tag{6}$$

If ε were made infinitesimally small, as prescribed by the standard scattering theory, then $G_\varepsilon(E)$ would coincide with the outgoing wave Green's operator $G(E)$ [see Eq. (8)], but Eq. (5) then would lead to the uncertainty $0\times\infty$. The trick of the approach proposed in [10,11] consists in *not* making ε infinitesimally small but assuming ε_a and ε_b to be finite non-negative functions of coordinates of the system having the meaning of *absorbing potentials*. This approach was successfully demonstrated by calculations for several three- [11–16] and even four-atomic [17] reaction systems; see, also, review articles [18]. However, the ambiguity in choosing the arbitrary functions ε_a and ε_b leaves something to be desired, as has been pointed out also by other authors [19]. This has motivated the present work whose goal is to show that the objectives of the theory of CRP mentioned above can be fully achieved by well-developed means of the standard scattering theory.

This paper is an outgrowth of our earlier Letter [20] whose principal results can be summarized as follows. In Ref. [20], we have derived a new formula for $N_{ab}(E)$ which in operator notation similarly to Eqs. (4) and (5) reads

$$N_{ab}(E)=\mathrm{tr}[F_a G(E)F_b G^*(E)]. \tag{7}$$

Here F_a and F_b are the flux operators in the arrangements a and b, respectively, and $G(E)$ is the outgoing wave Green's operator,

$$G(E)=(H-E-i0)^{-1}, \tag{8}$$

related to the microcanonical density operator $\delta(H-E)$ that appears in Eq. (4) by

$$\delta(H-E)=\frac{1}{\pi}\mathrm{Im}\,G(E). \tag{9}$$

It should be noted that the possibility to express the CRP without making an explicit reference to the asymptotic states and scattering matrix results from the following lucid physical picture underlying the present approach: rearrangement processes can be treated as a passage between two regions in configuration space. This also explains the appearance of flux operators in Eqs. (4) and (7). Such a viewpoint on rearrangement dynamics was adopted in the theory of chemical reactions since the early days of quantum mechanics [21]. In atomic physics, a formulation based on similar ideas was given by Gerjuoy [22] and, within impact parameter approach, by Demkov and Ostrovsky [23], see also Refs. [24,25]. Formula (7) is as an exact consequence of the Schrödinger equation as formula (4), both being equivalent to Eq. (3), but is more suitable for practical calculations. In order to implement Eq. (7), it is convenient to reduce the original multidimensional Schrödinger equation to a one-dimensional multichannel problem, which is a commonly used technique in quantum scattering calculations. Then, Eq. (7) takes a remarkably simple form [20],

$$N_{ab}(E)=\sum_{n_a,n_b}^{\mathrm{open}} k_{n_a}k_{n_b}|G_{n_a n_b}(E)|^2. \tag{10}$$

Here k_{n_a} and k_{n_b} are the channel momenta in the arrangements a and b, respectively, and $G_{n_a n_b}(E)$ are elements of the off-diagonal block of the matrix

$$\mathbf{G}(E)=2\mathcal{R}(\mathbf{I}-i\mathbf{k}\mathcal{R})^{-1}, \tag{11}$$

where $\mathbf{I}$ is the unit matrix, $\mathbf{k}$ is the diagonal matrix consisting of k_{n_a} and k_{n_b}, and $\mathcal{R}$ is the Wigner–Eisenbud $\mathcal{R}$ matrix

[26]. In Ref. [20], this approach was demonstrated by calculating the CRP for muon transfer reaction $d\mu+t\leftrightarrow d+t\mu$. In this paper, we give more details on the derivation of Eqs. (7), (10), and (11), which have been necessarily skipped in Ref. [20]. As the simplest model of reaction, first we consider a one-dimensional potential barrier problem (Sec. II). Then, we generalize this analysis to rearrangement collisions in three dimensions, adding a discussion of reaction eigenprobabilities introduced in Ref. [12] (Sec. III). In so doing, we employ a hyperspherical approach: this makes the derivation specific and related to the method used in the present calculations, however, it should be emphasized that this is not essential for the results represented by Eqs. (7), (10), and (11). Finally, the whole scheme is more intensively illustrated by calculations of two prototypical light atom transfer reactions in heavy-light-heavy triatomic systems $O(^3P)$-H-Cl and Br-H-Cl in three dimensions for zero total angular momentum (Sec. IV).

As it often happens, after publication of Ref. [20], we have learned that an approach close to ours, although only for the one-dimensional case, was considered earlier by Manolopoulos and Light [19]. In particular, equations similar to our Eqs. (7) and (10) are contained in Ref. [19]. We fully agree with the argumentation of these authors. The difference between our approaches in the one-dimensional case is minor; the only improvement we could add to their formulation is to use *Siegert pseudostates* [27,28] for expanding the outgoing wave Green's function, which has an advantage of reducing the computational labor needed to cover a wide energy range to a single matrix diagonalization (this development is discussed in the Appendix). At the same time, we believe that our implementation of Eq. (7) in terms of the $\mathcal{R}$ matrix for systems with many degrees of freedom is an important step forward. Indeed, the methods to calculate the $\mathcal{R}$ matrix are very well developed [29], so Eqs. (10) and (11) can be easily implemented on the basis of many existing quantum scattering codes.

Let us comment on convention adopted throughout this paper. We use mass-scaled coordinates, so masses of the particles participating in reaction will never appear in equations explicitly, but it is assumed that potential functions depend on them. To avoid possible ambiguities, we often show variables on which an operator acts explicitly as arguments of the operator in coordinate representation. If the operator depends on a parameter, this parameter may be also included in the list of arguments separated by a semicolon. Finally, we use a system of units where $\hbar=1$.

II. ONE-DIMENSIONAL MODEL

The purpose of this section is to introduce basic ideas of our approach by considering the simplest model of reaction, which is the problem of passing of a particle through a one-dimensional potential barrier. First, we derive Eqs. (7) and (10) for this case and then discuss their implementation. To make the parallelism explicit between the analysis of Sec. II A and its generalization to multidimensional case to be given in Sec. III B, we shall employ both coordinate representation and operator notation. The coordinate representation is the one which is actually used in the derivation, while in operator notation many of the equations take much simpler forms and remain almost unchanged in multidimensional case.

A. Derivation of the CRP in terms of the Green's function

The Schrödinger equation in the one-dimensional case reads

$$[H(x)-E]\psi(x)=0, \tag{12}$$

where $H(x)$ is the Hamiltonian

$$H(x)=-\frac{1}{2}\frac{d^2}{dx^2}+V(x). \tag{13}$$

In order to define the scattering matrix, we assume that the potential function $V(x)$ sufficiently rapidly approaches some constant values at $x\to\pm\infty$,

$$V(x)=V_a, \quad x\to-\infty, \tag{14a}$$

$$=V_b, \quad x\to+\infty. \tag{14b}$$

The asymptotic regions lying far on the left ($x\to-\infty$) and on the right ($x\to+\infty$) of the potential barrier will be associated with the arrangements a and b, respectively; we denote them by the same characters as the arrangements. The barrier itself will be associated with the reaction zone and denoted by I. Reaction amounts to passing of the particle from a to b or vice versa through I, which can occur at energies

$$E>\max(V_a,V_b). \tag{15}$$

For each energy in this range the following two degenerate solutions of Eq. (12) can be defined:

$$\psi_a(x)=\frac{e^{+ik_ax}}{\sqrt{k_a}}-S_{aa}(E)\frac{e^{-ik_ax}}{\sqrt{k_a}}, \quad x\to-\infty, \tag{16a}$$

$$=S_{ba}(E)\frac{e^{+ik_bx}}{\sqrt{k_b}}, \quad x\to+\infty, \tag{16b}$$

and

$$\psi_b(x)=S_{ab}(E)\frac{e^{-ik_ax}}{\sqrt{k_a}}, \quad x\to-\infty, \tag{17a}$$

$$=\frac{e^{-ik_bx}}{\sqrt{k_b}}-S_{bb}(E)\frac{e^{+ik_bx}}{\sqrt{k_b}}, \quad x\to+\infty. \tag{17b}$$

Here $S_{aa}(E)$, $S_{bb}(E)$, and $S_{ab}(E)=S_{ba}(E)$ are elements of the scattering matrix, and

$$k_{a,b}=\sqrt{2(E-V_{a,b})} \tag{18}$$

are the asymptotic values of the momentum. The CRP in the present case is defined by

$$N_{ab}(E)=|S_{ab}(E)|^2 \tag{19}$$

and coincides with the barrier transmission probability.

Let us introduce the outgoing wave Green's operator (8). Its action on a state vector $|\psi\rangle$ in coordinate representation is given by

$$G(E)|\psi\rangle=\int G(x,x';E)\psi(x')\,dx'. \tag{20}$$

Here the kernel $G(x,x';E)$, called the Green's function, satisfies the equation

$$[H(x)-E]G(x,x';E)=\delta(x-x') \tag{21}$$

and the outgoing wave boundary conditions

$$G(x,x';E)=c_a(x';E)e^{-ik_a x}, \quad x\to-\infty, \tag{22a}$$

$$=c_b(x';E)e^{+ik_b x}, \quad x\to+\infty, \tag{22b}$$

where $c_a(x';E)$ and $c_b(x';E)$ are certain functions. In the present case, the Green's function can be expressed in terms of the solutions $\psi_a(x)$ and $\psi_b(x)$,

$$G(x,x';E)=\frac{i}{S_{ab}}\psi_a(x_>)\psi_b(x_<), \tag{23}$$

where $x_>$ ($x_<$) is the larger (the smaller) of x and x'. However, there is not an analog of this equation in multidimensional case, so we shall not use it in the derivation. The microcanonical density operator (9) also can be expressed in terms of these solutions,

$$\delta(H-E)=\frac{1}{2\pi}(|\psi_a\rangle\langle\psi_a|+|\psi_b\rangle\langle\psi_b|), \tag{24}$$

which does have a generalization in multidimensional case.

We now introduce the operator of flux at the point q,

$$F(x;q)=\frac{1}{2i}\left[\delta(x-q)\frac{d}{dx}+\frac{d}{dx}\delta(x-q)\right], \tag{25}$$

Its matrix elements between any two state vectors $|\psi_1\rangle$ and $|\psi_2\rangle$ are given by

$$\langle\psi_1|F(q)|\psi_2\rangle=\int\psi_1^*(x)F(x;q)\psi_2(x)dx$$
$$=\frac{1}{2i}\left(\psi_1^*(q)\frac{d\psi_2(q)}{dq}-\frac{d\psi_1^*(q)}{dq}\psi_2(q)\right). \tag{26}$$

If $|\psi_1\rangle$ and $|\psi_2\rangle$ are solutions of Eq. (12), then it can be easily shown that

$$\frac{d}{dq}\langle\psi_1|F(q)|\psi_2\rangle=0. \tag{27}$$

In particular, using the boundary conditions (16b) and (17a), we obtain

$$\langle\psi_a|F(q)|\psi_a\rangle=-\langle\psi_b|F(q)|\psi_b\rangle=|S_{ab}(E)|^2. \tag{28}$$

The combined action of first $F(q)$ and then $G(E)$ on a state vector $|\psi\rangle$ in coordinate representation is given by

$$G(E)F(q)|\psi\rangle=\frac{1}{2i}\left(G(x,q;E)\frac{d\psi(q)}{dq}-\frac{\partial G(x,q;E)}{\partial q}\psi(q)\right). \tag{29}$$

The key role in the derivation of Eq. (7) belongs to the Green's formula. This formula can be obtained by substituting in Eq. (12) x' instead of x, multiplying from the left by $G(x,x';E)$, integrating over $x'\in[x_a,x_b]$, and using Eq. (21). Taking into account Eq. (29), the result can be presented in the form

$$iG(E)[F(x_b)-F(x_a)]|\psi\rangle=\theta(x-x_a)\theta(x_b-x)\psi(x). \tag{30}$$

Substituting here $|\psi_a\rangle$ [$|\psi_b\rangle$] instead of $|\psi\rangle$, putting $x_b\to+\infty$ [$x_a\to-\infty$], and using the boundary conditions (16b) and (22b) [(17a) and (22a)], we obtain

$$-iG(E)F(q)|\psi_a\rangle=\theta(x-q)\psi_a(x), \tag{31a}$$

$$+iG(E)F(q)|\psi_b\rangle=\theta(q-x)\psi_b(x). \tag{31b}$$

Vanishing of the right-hand side of Eq. (31a) [Eq. (31b)] at $x<q$ [$x>q$] indicates the fact that both Green's function $G(x,x';E)$ and solution $\psi_a(x)$ [$\psi_b(x)$] have only outgoing waves in the region b [a], thus they are linearly dependent there. Quite similarly one can obtain

$$iG(E)F(q)G(E)=[\theta(q-x)-\theta(q-x')]G(x,x';E), \tag{32}$$

where the right-hand side is the kernel of the operator standing on the left-hand side.

Let us turn to the derivation of Eq. (7). Using Eqs. (19) and (28), the CRP can be identified with the flux in the state $|\psi_a\rangle$,

$$N_{ab}(E)=\langle\psi_a|F(q)|\psi_a\rangle, \tag{33}$$

where q is arbitrary. Using Eq. (31a) we can rewrite this as follows:

$$\theta(q-q')N_{ab}(E)=-i\langle\psi_a|F(q)G(E)F(q')|\psi_a\rangle. \tag{34}$$

Acting similarly, but now identifying the CRP with the negative of the flux in the state $|\psi_b\rangle$ and using Eq. (31b), we have

$$\theta(q'-q)N_{ab}(E)=-i\langle\psi_b|F(q)G(E)F(q')|\psi_b\rangle. \tag{35}$$

Adding Eqs. (34) and (35) and taking into account Eq. (24), we obtain

$$N_{ab}(E)=-2\pi i\ \mathrm{tr}[F(q)G(E)F(q')\delta(H-E)]. \tag{36}$$

As follows from Eq. (32),

$$\mathrm{tr}[F(q)G(E)F(q')G(E)]=0, \tag{37}$$

thus Eq. (36) can be cast in the form

$$N_{ab}(E)=\mathrm{tr}[F(q)G(E)F(q')G^*(E)]. \tag{38}$$

Taking separately real and imaginary parts of Eq. (37), from Eq. (36) we obtain two more representations for $N_{ab}(E)$:

$$N_{ab}(E)=2\pi^2\ \mathrm{tr}[F(q)\,\delta(H-E)F(q')\,\delta(H-E)] \tag{39}$$

and

$$N_{ab}(E)=2\ \mathrm{tr}[F(q)\mathrm{Re}\ G(E)F(q')\mathrm{Re}\ G(E)]. \tag{40}$$

Equation (38) coincides with our main formula (7); Eq. (39) coincides with the MST formula (4); while Eqs. (36) and (40), to our knowledge, have not yet appeared in literature. We shall not discuss derivation of Eq. (5), since this would require introducing absorbing potentials, but this formula can be easily obtained from the above equations.

We now show that among Eqs. (36) and (38)–(40) the second one is most convenient for implementation. To this end let us rewrite it in coordinate representation:

$$\begin{aligned}N_{ab}(E)=-\frac{1}{4}\Bigg[&\frac{\partial G(q,q';E)}{\partial q}\,\frac{\partial G^*(q,q';E)}{\partial q'}\\&+\frac{\partial G(q,q';E)}{\partial q'}\,\frac{\partial G^*(q,q';E)}{\partial q}\\&-\frac{\partial^2 G(q,q';E)}{\partial q\,\partial q'}G^*(q,q';E)\\&-G(q,q';E)\frac{\partial^2 G^*(q,q';E)}{\partial q\,\partial q'}\Bigg].\end{aligned} \tag{41}$$

This equation specifies the meaning of formula (7) for the one-dimensional case. Here q and q' are arbitrary, but the case $q=q'$, if desired, should be understood as one of the limits $q\to q'\pm 0$ (both limits give identical results), since the derivatives of the Green's function $G(q,q';E)$ that appear in Eq. (41) are not defined at $q=q'$. This remark applies also to Eqs. (36), (39), and (40) and becomes important if in implementing these equations one takes both flux operators on a *single* ''dividing surface,'' as is usually done in literature where the MST formula (4) is used. For example, taking the limit $q=q'$ in Eq. (39) improperly was the reason of some artificial difficulties encountered in Ref. [30]. In our approach, we take the flux operators on *two different* surfaces, namely, on the boundaries between the reaction zone I and the regions occupied by the arrangements a and b. Using the arbitrariness of q and q' in Eq. (41), we put $q=x_a\to-\infty$ and $q'=x_b\to+\infty$. Then, taking into account the boundary conditions (22) for the Green's function, we obtain

$$N_{ab}(E)=k(x_a)k(x_b)\left|G(x_a,x_b;E)\right|^2\Big|_{x_a\to-\infty}^{x_b\to+\infty}, \tag{42}$$

where

$$k(x)=\sqrt{2[E-V(x)]}. \tag{43}$$

Equation (42) specifies the meaning of Eq. (10) for the one-dimensional case. Assuming x_a and x_b to be large but finite amounts to imposing the outgoing wave boundary conditions (22) semiclassically. This accelerates convergence of the results as the size of the reaction zone $I=[x_a,x_b]$ grows and makes our approach practical. Note that no such a simple formula can be obtained on the basis of Eq. (36), (39), or (40).

Before we further proceed, it is worthwhile to point out one interesting aspect of the CRP revealed by the above equations. Let us calculate the total flux $\mathcal{J}$ at the point q in a mixed state defined by the microcanonical density operator (24). As follows from Eq. (28), in the unperturbed system $\mathcal{J}=0$. Consider a perturbation of the Hamiltonian (13),

$$\delta H=\mathcal{F}L(q'),\quad L(q')=iF(q'), \tag{44}$$

where $\mathcal{F}$ is a small real constant and $L(q')$ coincides with the Bloch operator at the point q' [31]. Note that δH is a skew Hermitian operator, i.e., $\delta H^\dagger=-\delta H$. Using the Kubo's linear response theory [5] and Eq. (36), for the perturbed system in the first order with respect to $\mathcal{F}$ we obtain

$$\mathcal{J}=\frac{N_{ab}(E)}{\pi}\mathcal{F}. \tag{45}$$

The perturbation operator (44) acts as a pump introduced at the point q'. Indeed, it can be shown that it produces discontinuities in the values of flux in the perturbed states $\psi_a(x)$ and $\psi_b(x)$ at $x=q'$. As follows from Eq. (45), $N_{ab}(E)/\pi$ can be interpreted as the corresponding response function in the state of microcanonical equilibrium. This interpretation explains why the CRP can be expressed in terms of the Green's function alone.

B. Construction of the Green's function

To implement Eq. (42), one has to construct the Green's function $G(x,x';E)$ with its two arguments lying in the regions occupied by the arrangements a and b. This is a separate problem and it can be solved by various methods. For example, one could use absorbing potentials as a means to implicitly impose the outgoing wave boundary conditions, provided that they do not disturb the dynamics inside the reaction zone and do not cause reflection, in other words, provided that a sufficient experience in working with such a device is developed. However we prefer to impose the outgoing wave boundary conditions explicitly. Here we describe a method for constructing the Green's function which is straightforward and consistent with the spirit of the present approach and with scattering theory.

We assume that for a given energy E the reaction zone I is confined to the interval $[x_a,x_b]$, i.e., that only this interval is essential for calculating $N_{ab}(E)$. Then the boundary conditions (22) can be approximated semiclassically,

$$\left[\frac{\partial}{\partial x}+ik(x_a)\right]G(x,x';E)\big|_{x=x_a}=0, \tag{46a}$$

$$\left[\frac{\partial}{\partial x}-ik(x_b)\right]G(x,x';E)|_{x=x_b}=0. \tag{46b}$$

Let us introduce a complete and orthonormal basis in the interval $I=[x_a,x_b]$:

$$\int_{x_a}^{x_b}\pi_i(x)\pi_j(x)dx=\delta_{ij}. \tag{47}$$

Then the Green's function $G(x,x';E)$ for both x and x' inside I can be expanded as

$$G(x,x';E)=\sum_{i,j}G_{ij}\pi_i(x)\pi_j(x'). \tag{48}$$

Substituting this into Eq. (21), multiplying from the left by $\pi_i(x)\pi_j(x')$, integrating over $x\in I$ and $x'\in I$, and using Eqs. (46), for the matrix $\mathbf{G}$ of coefficients G_{ij} we obtain

$$\left(\tilde{\mathbf{H}}-\frac{i}{2}[k(x_a)\mathbf{L}(x_a)+k(x_b)\mathbf{L}(x_b)]-E\mathbf{I}\right)\mathbf{G}=\mathbf{I}. \tag{49}$$

Here $\tilde{\mathbf{H}}$ represents the Hermitian part of the Hamiltonian (13),

$$\tilde{H}_{ij}=\frac{1}{2}\int_{x_a}^{x_b}\frac{d\pi_i(x)}{dx}\frac{d\pi_j(x)}{dx}dx+\int_{x_a}^{x_b}\pi_i(x)V(x)\pi_j(x)dx, \tag{50}$$

and $\mathbf{L}(x)$ is defined by

$$L_{ij}(x)=\pi_i(x)\pi_j(x), \tag{51}$$

so that the second term in Eq. (49) is a matrix representation of the Bloch operator for the solutions satisfying outgoing wave boundary conditions. Thus the problem of constructing the Green's function is reduced to inversion of the matrix multiplying $\mathbf{G}$ in Eq. (49). This can be easily done for any reasonable one-dimensional potential satisfying Eq. (14). However, in multidimensional case, the size of the basis may become too large and this straightforward procedure may become unfeasible. In Sec. III D, we describe a more powerful approach to constructing the Green's function which remains feasible in more general situations.

The outlined above procedure is similar to that used by Manolopoulos and Light [19], so we shall not discuss here its numerical illustrations. The only difference is that these authors basing on semiclassical arguments have included an additional term proportional to $dV(x)/dx$ in the boundary conditions (46), which we found to be not essential. But we would like to repeat here and to emphasize the principal conclusion made in Ref. [19] and confirmed by our calculations: Equation (42) enables one to calculate $N_{ab}(E)$ with the required accuracy by considering an interval of x as much as three times smaller than that which has to be considered using the best of absorbing potentials [10]. A more elegant and much more efficient implementation of our approach, in terms of Siegert pseudostates is discussed for the case of symmetric potentials in the Appendix.

III. REARRANGEMENT PROCESSES: HYPERSPHERICAL FORMULATION

A. Preliminary remarks on the hyperspherical treatment of collisions in few-body systems

Consider a system of $N\geqslant 3$ structureless particles whose potential energy is a given function of the particles' relative position. Let m_i be the mass of the ith particle and $\mathbf{r}_i$ be its coordinate in the center-of-mass frame. With the center-of-mass motion separated out, configuration space of such system has the dimension $d=3(N-1)$. It can be parametrized by a set of $N-1$ three-dimensional mass-scaled Jacobi vectors $\mathbf{x}_i$ defined as such linear combinations of $\mathbf{r}_i$ that the kinetic energy of the system expressed in terms of $\mathbf{x}_i$ is given by

$$T=-\frac{1}{2}\sum_{i=1}^{N-1}\Delta(\mathbf{x}_i). \tag{52}$$

This equation does not define the Jacobi vectors uniquely. In fact, there is an infinity of Jacobi sets satisfying Eq. (52) and related to each other by kinematic rotations. A finite number of them enjoying an additional property that each vector $\mathbf{x}_i$ joins centers of mass of two groups of particles are most frequently used in applications; see, e.g., Ref. [32]. An alternative parametrization of configuration space and the one employed in hyperspherical approach is obtained by considering $\mathbf{x}_i$ as orthogonal components of a single d-dimensional vector $\mathbf{R}=(\mathbf{x}_1,\ldots,\mathbf{x}_{N-1})$ and introducing hyperspherical coordinates $\mathbf{R}=(R,\Omega)$, where the hyperradius R is the length of $\mathbf{R}$,

$$R^2=\sum_{i=1}^{N-1}\mathbf{x}_i^2=\sum_{i=1}^{N}m_i\mathbf{r}_i^2, \tag{53}$$

and Ω is a collective notation for a set of $3N-4$ hyperspherical angles parametrizing hypersphere which we denote by $\mathcal{S}$. This set can be further specified as $\Omega=(\Omega_s,\Omega_o)$, where Ω_s denotes a set of $3N-7$ ''shape'' angles defining the relative position of particles for a given R, and Ω_o denotes a set of three angles defining the overall orientation of the system for given R and Ω_s, e.g., three Euler angles. The Schrödinger equation in hyperspherical coordinates reads

$$[\tilde{H}(\mathbf{R})-E]\tilde{\psi}(\mathbf{R})=0, \tag{54}$$

where

$$\tilde{H}(\mathbf{R})=-\frac{1}{2}\Delta(\mathbf{R})+V(R,\Omega_s), \tag{55}$$

and it is explicitly shown that the potential energy does not depend on orientational angles. By writing the Schrödinger equation in this form, the N-body problem in three-dimensional space is formally reduced to the problem of scattering of one ''particle'' representing the whole system by the potential field $V(R,\Omega_s)$ in d-dimensional space. Such a reduction has the advantage of laying grounds for new powerful methods of constructing the wave function that are

capable to provide a unified description of different types of collision processes [33]. Indeed, the high efficiency of hyperspherical approach was demonstrated by applications to various nuclear, atomic, and molecular few-body problems. However, it should be noted that the majority of these applications is restricted to the energy range below the three-fragment disintegration threshold. The extension of hyperspherical approach to higher energies meets difficulties associated with the possibility for the system to disintegrate into three or more fragments which prevents obtaining a uniform asymptotic of the wave function at $R\to\infty$ valid over entire hypersphere $\mathcal{S}$, which is needed for formulating the asymptotic boundary conditions. Even for the three-body systems, in which case some rigorous mathematical results in this direction do exist [32], their usefulness for practical calculations is still very limited. Consequently, in the following we restrict ourselves to considering only rearrangement collisions with two fragments in both initial and final states of the system. If the particles involved are atoms and $V(R,\Omega_s)$ is an electronically adiabatic potential energy surface (PES) obtained by averaging out the electronic degrees of freedom, then Eq. (54) provides a model to describe chemical reactions. The above restriction then means that only bimolecular reactions will be considered in this paper.

B. Derivation of the CRP in terms of the Green's function

For our purposes, it is convenient to introduce a new function,

$$\psi(\mathbf{R})=R^{(d-1)/2}\tilde{\psi}(\mathbf{R}), \tag{56}$$

and to rewrite Eq. (54) as

$$[H(\mathbf{R})-E]\psi(\mathbf{R})=0, \tag{57}$$

where

$$H(\mathbf{R})=-\frac{1}{2}\frac{\partial^2}{\partial R^2}+\frac{H_{\rm ad}(\Omega;R)+\frac{1}{8}(d-1)(d-3)}{R^2}. \tag{58}$$

Here

$$H_{\rm ad}(\Omega;R)=\frac{1}{2}\Lambda^2(\Omega)+R^2V(R,\Omega_s) \tag{59}$$

is the hyperspherical adiabatic (HSA) Hamiltonian defining the motion of the system on the hypersphere of radius R, and $\Lambda^2(\Omega)$ is the grand angular momentum operator squared whose particular expression is not needed for the present discussion. In hyperspherical approach the solutions to Eq. (57) are sought in the form [34]

$$\psi(\mathbf{R})=\sum_n F_n(R)\Phi_n(\Omega;R). \tag{60}$$

Here the angular dependence of $\psi(\mathbf{R})$ is represented by the solutions of the HSA eigenvalue problem,

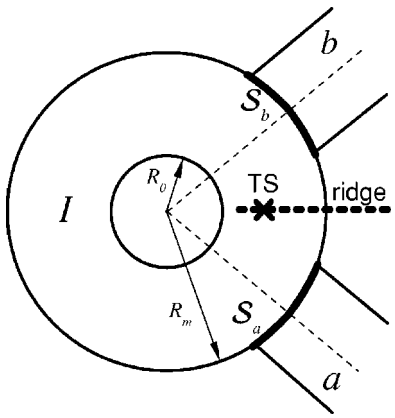

FIG. 1. Sketch of the region of configuration space where the reaction between arrangements a and b takes place; see text for further explanations.

$$\left[H_{\rm ad}(\Omega;R)+\frac{1}{8}(d-1)(d-3)-R^2U_n(R)\right]\Phi_n(\Omega;R)=0, \tag{61}$$

where $U_n(R)$ and $\Phi_n(\Omega;R)$ are called the HSA potentials and channel functions, respectively. For any R, functions $\Phi_n(\Omega;R)$, $n=1,2,\ldots$, form a complete and orthogonal basis on $\mathcal{S}$ which we assume to be normalized by

$$\int_{\mathcal{S}}\Phi_n(\Omega;R)\Phi_{n'}(\Omega;R)d\Omega=\delta_{nn'}. \tag{62}$$

The radial functions $F_n(R)$ in Eq. (60) satisfy a set of ordinary differential equations,

$$\left[-\frac{1}{2}\frac{d^2}{dR^2}+U_n(R)-E\right]F_n(R)=\sum_n W_{nn'}(R)F_{n'}(R), \tag{63}$$

where $W_{nn'}(R)$ is the operator of nonadiabatic coupling between different HSA channels whose particular form also is not needed for the present discussion (see, e.g., Ref. [34]).

Suppose there are several (more than one) ways for the system to disintegrate into two bound clusters. The different modes of such disintegration will be called arrangements and will be denoted by the lower case characters $a=A_1+A_2$, $b=B_1+B_2$, etc., where the upper case characters denote the corresponding clusters. For simplicity of the derivation we consider only one pair of arrangements, a and b, and discuss the rearrangement process

$$A_1+A_2\leftrightarrow B_1+B_2. \tag{64}$$

Any other pair can be treated in a similar way. For the following analysis it is important to realize the structure of the region of configuration space where reaction (64) takes place. This region approximately coincides with the classically accessible region defined by $E>V(R,\Omega_s)$ and is schematically shown in Fig. 1. In hyperspherical approach, each arrangement is represented by states localized in a separate valley of the potential function $V(R,\Omega_s)$. These valleys ex-

tend along certain directions to the asymptotic region $R \to \infty$ and are indicated in the figure by the names of the corresponding arrangements. At large R, the valleys a and b are well separated by a potential ridge shown by the thick dashed line; here the arrangements are distinct. At smaller R, the height and the width of the ridge gradually decrease, and it eventually disappears somewhere in the vicinity of the transition state for reaction (64) indicated in the figure by the cross. Here the valleys a and b merge with each other and with valleys representing other arrangements, if any (not shown in the figure), forming a common potential well where partitioning of the system into separate fragments loses its meaning. This region will be called the reaction zone and denoted by I. Reaction (64) amounts to passing of the system from the valley a to the valley b or vice versa through the reaction zone I. At even smaller R, where all particles are close together, there may be a hard core produced by the repulsive part of the interparticle interactions, as in the case of interatomic potentials. Particles do not penetrate here, so this region can be excluded from the consideration. The possibility to trace transitions between the different regions by variation of a single variable R is another advantage of hyperspherical approach.

Let us define the regions discussed above more precisely. We represent the hard core by the interior of the hypersphere of radius R_0 and assume that

$$\psi(\mathbf{R}) = 0, \quad 0 \leqslant R \leqslant R_0. \tag{65}$$

In the following, only the region $R \geqslant R_0$ will be considered. The reaction zone I is identified with the hyperspherical shell lying in the interval $R_0 < R < R_m$, where R_m will be called the matching radius. The directions along which the valleys a and b extend are defined as follows. Consider, e.g., the arrangement a. Let $\mathbf{x}_1^a, \ldots, \mathbf{x}_{N-1}^a$ be such a Jacobi set that each vector $\mathbf{x}_i^a$ is a linear combination of coordinates of particles belonging to the same cluster, either A_1 or A_2, except the last vector $\mathbf{x}_{N-1}^a$ which joins the centers of mass of the clusters. Let α_a be defined by

$$R \cos \alpha_a = x_{N-1}^a, \quad R \sin \alpha_a = \left(\sum_{i=1}^{N-2} (\mathbf{x}_i^a)^2 \right)^{1/2}, \tag{66}$$

$$0 \leqslant \alpha_a \leqslant \pi/2.$$

Equation $\alpha_a = 0$ defines a point in the space of shape angles Ω_s which, taking into account the rotational degrees of freedom, corresponds to a three-dimensional manifold belonging to hypersphere $\mathcal{S}$. The orbit of this manifold as R varies is the *hyperaxis* of the valley a. The hyperaxis of the valley b can be defined similarly by the equation $\alpha_b = 0$. These hyperaxes are shown by the thin dashed lines in Fig. 1. The valleys a and b are *hypercylindrical* regions around these hyperaxes. The boundaries between a and b and the reaction zone I, indicated in the figure by $\mathcal{S}_a$ and $\mathcal{S}_b$, are nonoverlapping segments of the hypersphere of radius R_m. They can be defined in terms of the HSA channel functions $\Phi_n(\Omega;R)$. Let $\overline{E}$ be the three-fragment disintegration threshold energy. For any $E < \overline{E}$, there is only a finite number of open channels in each of the arrangements a and b; let us enumerate them by the indices n_a and n_b, respectively. At $R \to \infty$ functions $\Phi_{n_a}(\Omega;R)$ $[\Phi_{n_b}(\Omega;R)]$ are localized on hypersphere near the direction $\alpha_a = 0$ $[\alpha_b = 0]$. Hence, for sufficiently large $R = R_m$ the region of integration in Eq. (62) for the case if both channels n and n' belong to the same arrangement a (b) can be reduced from entire hypersphere $\mathcal{S}$ to a segment $\mathcal{S}_a$ $(\mathcal{S}_b)$ centered at $\alpha_a = 0$ $[\alpha_b = 0]$:

$$\int_{\mathcal{S}_a} \Phi_{n_a}(\Omega_a;R_m)\Phi_{n_a'}(\Omega_a;R_m)\,d\Omega_a = \delta_{n_a n_a'}, \tag{67a}$$

$$\int_{\mathcal{S}_b} \Phi_{n_b}(\Omega_b;R_m)\Phi_{n_b'}(\Omega_b;R_m)\,d\Omega_b = \delta_{n_b n_b'}. \tag{67b}$$

The requirement that these equations must hold with a specified accuracy for all the open channels defines the segments $\mathcal{S}_a$ and $\mathcal{S}_b$, while the condition that $\mathcal{S}_a$ and $\mathcal{S}_b$ do not overlap sets a lower boundary on the admissible values of the matching radius R_m. In the following, we shall assume that the parameters R_0 and R_m in the described construction are chosen to minimize the size of the reaction zone I, provided that Eqs. (65) and (67) are satisfied and the segments $\mathcal{S}_a$ and $\mathcal{S}_b$ do not overlap. It should be understood that these parameters depend on energy, and that when using a nonzero R_0 and a finite R_m, one must demonstrate convergence of the results as $R_0 \to 0$ and $R_m \to \infty$.

At $R \to \infty$ the HSA potentials corresponding to the open channels in the arrangements a and b approach some constant values,

$$U_{n_{a,b}}(R) = E_{n_{a,b}}, \quad R \to \infty, \tag{68}$$

and the nonadiabatic coupling terms in Eq. (63) can be neglected. Let $E_a = \min\{E_{n_a}\}$ and $E_b = \min\{E_{n_b}\}$. The following discussion of reaction (64) applies to the energy range

$$\max(E_a, E_b) < E < \overline{E}. \tag{69}$$

For each energy in this interval, the following degenerate solutions of Eq. (57) similar to that given by Eqs. (16) and (17) for the one-dimensional case can be defined:

$$\psi_{n_a}(\mathbf{R}) = \frac{e^{-ik_{n_a}R}}{\sqrt{k_{n_a}}}\Phi_{n_a}(\Omega;R) - \sum_{n_a'}^{\text{open}} S_{n_a' n_a}(E)\frac{e^{+ik_{n_a'}R}}{\sqrt{k_{n_a'}}}\Phi_{n_a'}(\Omega;R),$$

$$\mathbf{R} \in a \quad \text{and } R \to \infty, \tag{70a}$$

$$= \sum_{n_b}^{\text{open}} S_{n_b n_a}(E)\frac{e^{+ik_{n_b}R}}{\sqrt{k_{n_b}}}\Phi_{n_b}(\Omega;R),$$

$$\mathbf{R} \in b \text{ and } R \to \infty, \tag{70b}$$

and

$$\psi_{n_b}(\mathbf{R}) = \sum_{n_a}^{\text{open}} S_{n_a n_b}(E) \frac{e^{+ik_{n_a}R}}{\sqrt{k_{n_a}}} \Phi_{n_a}(\Omega;R), \quad \mathbf{R} \in a \ \text{ and } R \to \infty, \tag{71a}$$

$$= \frac{e^{-ik_{n_b}R}}{\sqrt{k_{n_b}}} \Phi_{n_b}(\Omega;R) - \sum_{n_b'}^{\text{open}} S_{n_b' n_b}(E) \frac{e^{+ik_{n_b'}R}}{\sqrt{k_{n_b'}}} \Phi_{n_b'}(\Omega;R), \quad \mathbf{R} \in b \ \text{ and } R \to \infty. \tag{71b}$$

Here $S_{n_a n_a'}(E)$, $S_{n_b n_b'}(E)$, and $S_{n_a n_b}(E) = S_{n_b n_a}(E)$ are elements of the scattering matrix (2), and

$$k_{n_{a,b}} = \sqrt{2(E - E_{n_{a,b}})} \tag{72}$$

are the asymptotic values of the open channel momenta. The CRP is defined in terms of the scattering matrix by Eq. (3).

The following development parallels that of Sec. II A. We introduce the outgoing wave Green's operator (8). Its action on a state vector $|\psi\rangle$ in coordinate representation is given by

$$G(E)|\psi\rangle = \int G(\mathbf{R},\mathbf{R}';E)\psi(\mathbf{R}')dR'd\Omega'. \tag{73}$$

The Green's function $G(\mathbf{R},\mathbf{R}';E)$ satisfies the equation

$$[H(\mathbf{R}) - E]G(\mathbf{R},\mathbf{R}';E) = \delta(R - R')\delta(\Omega - \Omega') \tag{74}$$

and the outgoing wave boundary conditions

$$G(\mathbf{R},\mathbf{R}';E) = \sum_{n_a}^{\text{open}} c_{n_a}(\mathbf{R}';E) \frac{e^{+ik_{n_a}R}}{\sqrt{k_{n_a}}} \Phi_{n_a}(\Omega;R), \quad \mathbf{R} \in a \ \text{ and } R \to \infty, \tag{75a}$$

$$= \sum_{n_b}^{\text{open}} c_{n_b}(\mathbf{R}';E) \frac{e^{+ik_{n_b}R}}{\sqrt{k_{n_b}}} \Phi_{n_b}(\Omega;R), \quad \mathbf{R} \in b \text{ and } R \to \infty, \tag{75b}$$

where $c_{n_a}(\mathbf{R}';E)$ and $c_{n_b}(\mathbf{R}';E)$ are certain functions. The microcanonical density operator (9) is expressed in terms of the solutions $\psi_{n_a}(\mathbf{R})$ and $\psi_{n_b}(\mathbf{R})$ by

$$\delta(H - E) = \frac{1}{2\pi}\left(\sum_{n_a}^{\text{open}} |\psi_{n_a}\rangle\langle\psi_{n_a}| + \sum_{n_b}^{\text{open}} |\psi_{n_b}\rangle\langle\psi_{n_b}| \right). \tag{76}$$

Let us introduce the operator of flux through the hypersphere of radius Q,

$$F(R;Q) = \frac{1}{2i}\left[\delta(R - Q)\frac{\partial}{\partial R} + \frac{\partial}{\partial R}\delta(R - Q) \right], \tag{77}$$

Its matrix elements between any two state vectors $|\psi_1\rangle$ and $|\psi_2\rangle$ are given by

$$\langle\psi_1|F(Q)|\psi_2\rangle = \int \psi_1^*(\mathbf{R})F(R;Q)\psi_2(\mathbf{R})dRd\Omega = \frac{1}{2i}\int_{\mathcal{S}}\left(\psi_1^*(\mathbf{Q})\frac{\partial\psi_2(\mathbf{Q})}{\partial Q} - \frac{\partial\psi_1^*(\mathbf{Q})}{\partial Q}\psi_2(\mathbf{Q}) \right) d\Omega, \tag{78}$$

where $\mathbf{Q} = (Q,\Omega)$. If $|\psi_1\rangle$ and $|\psi_2\rangle$ are solutions of Eq. (57), then it can be shown that

$$\langle\psi_1|F(Q)|\psi_2\rangle = 0. \tag{79}$$

Substituting here $|\psi_{n_a}\rangle$ or $|\psi_{n_b}\rangle$ instead of $|\psi_1\rangle$ and $|\psi_2\rangle$, putting $Q \to \infty$ and using the boundary conditions (70) and (71) and Eq. (62), we obtain

$$\sum_{n_a'}^{\text{open}} |S_{n_a' n_a}(E)|^2 + \sum_{n_b}^{\text{open}} |S_{n_b n_a}(E)|^2 = 1, \tag{80a}$$

$$\sum_{n_b'}^{\text{open}} |S_{n_b' n_b}(E)|^2 + \sum_{n_a}^{\text{open}} |S_{n_a n_b}(E)|^2 = 1. \tag{80b}$$

This establishes unitarity of the scattering matrix. In addition, we introduce the flux operators separately for each of the arrangements. Let $\mathcal{S}_a$ ($\mathcal{S}_b$) be the segment of the hypersphere of some large radius R_a (R_b) lying in the valley a (b). (Here, for the purpose of derivation, we temporarily deviate from the previous definition of $\mathcal{S}_a$ and $\mathcal{S}_b$, but we shall return to it shortly). In the following, it will be assumed that $R_a \geqslant R_m$ and $R_b \geqslant R_m$. We define the operators of flux through the segments $\mathcal{S}_a$ and $\mathcal{S}_b$:

$$\langle\psi_1|F_a(R_a)|\psi_2\rangle = \frac{1}{2i}\int_{\mathcal{S}_a}\left(\psi_1^*(\mathbf{R}_a)\frac{\partial\psi_2(\mathbf{R}_a)}{\partial R_a} - \frac{\partial\psi_1^*(\mathbf{R}_a)}{\partial R_a}\psi_2(\mathbf{R}_a) \right) d\Omega_a, \tag{81a}$$

$$\langle\psi_1|F_b(R_b)|\psi_2\rangle = \frac{1}{2i}\int_{\mathcal{S}_b}\left(\psi_1^*(\mathbf{R}_b)\frac{\partial\psi_2(\mathbf{R}_b)}{\partial R_b} - \frac{\partial\psi_1^*(\mathbf{R}_b)}{\partial R_b}\psi_2(\mathbf{R}_b) \right) d\Omega_b. \tag{81b}$$

If $|\psi_1\rangle$ and $|\psi_2\rangle$ are solutions of Eq. (57), then it can be shown that the left hand sides of these equations do not depend on R_a and R_b. In particular, using the boundary conditions (70) and (71) and Eqs. (67), we obtain

$$\langle\psi_{n_a}|F_b(R_b)|\psi_{n_a}\rangle = \sum_{n_b}^{\text{open}} |S_{n_b n_a}(E)|^2, \tag{82a}$$

$$\langle \psi_{n_b}|F_a(R_a)|\psi_{n_b}\rangle = \sum_{n_a}^{\text{open}} |S_{n_a n_b}(E)|^2. \tag{82b}$$

The combined action of first $F(Q)$ and then $G(E)$ on a state vector $|\psi\rangle$ in coordinate representation is given by

$$G(E)F(Q)|\psi\rangle = \frac{1}{2i}\int_{\mathcal{S}}\left(G(\mathbf{R},\mathbf{Q};E)\frac{\partial\psi(\mathbf{Q})}{\partial Q} - \frac{\partial G(\mathbf{R},\mathbf{Q};E)}{\partial Q}\psi(\mathbf{Q})\right) d\Omega, \tag{83}$$

and similarly for $F_a(R_a)$ and $F_b(R_b)$ with $\mathcal{S}$ replaced by $\mathcal{S}_a$ and $\mathcal{S}_b$, respectively.

Again our derivation of Eq. (7) is based on the Green's formula. This can be obtained by substituting in Eq. (57) $\mathbf{R}'$ instead of $\mathbf{R}$, multiplying from the left by $G(\mathbf{R},\mathbf{R}';E)$, integrating over $R' \in [R_0, Q]$ and $\Omega' \in \mathcal{S}$, and using Eq. (74). Taking into account Eq. (83), the result can be presented in the form

$$iG(E)[F(Q)-F(R_0)]|\psi\rangle = \theta(Q-R)\psi(\mathbf{R}). \tag{84}$$

Because of the boundary condition (65), the term with $F(R_0)$ vanishes. Substituting here $|\psi_{n_a}\rangle$ $[|\psi_{n_b}\rangle]$ instead of $|\psi\rangle$ and putting $Q=R_a$ $(Q=R_b)$ we obtain

$$iG(E)F_a(R_a)|\psi_{n_a}\rangle = \theta(R_a-R)\psi_{n_a}(\mathbf{R}), \tag{85a}$$

$$iG(E)F_b(R_b)|\psi_{n_b}\rangle = \theta(R_b-R)\psi_{n_b}(\mathbf{R}). \tag{85b}$$

Vanishing of the right hand side of Eq. (85a) [Eq. (85b)] at $R>R_a$ $[R>R_b]$ indicates the fact that both Green's function $G(\mathbf{R},\mathbf{R}';E)$ and solutions $\psi_{n_a}(\mathbf{R})$ $[\psi_{n_b}(\mathbf{R})]$ have only outgoing waves in the valley b (a), thus they are linearly dependent there. Quite similarly we obtain

$$iG(E)F(Q)G(E) = [\theta(Q-R)-\theta(Q-R')]G(\mathbf{R},\mathbf{R}';E), \tag{86}$$

where the right-hand side is the kernel of the operator standing on the left-hand side.

We now turn to the derivation of Eq. (7). Using Eqs. (3) and (82a), the CRP can be identified with the total flux in all open channels of the arrangement a in the valley b,

$$N_{ab}(E) = \sum_{n_a}^{\text{open}} \langle \psi_{n_a}|F_b(R_b)|\psi_{n_a}\rangle. \tag{87}$$

Using Eq. (85a) we can rewrite this as

$$\theta(R_a-R_b)N_{ab}(E) = i\sum_{n_a}^{\text{open}} \langle \psi_{n_a}|F_b(R_b)G(E)F_a(R_a)|\psi_{n_a}\rangle. \tag{88}$$

Acting similarly, but now identifying the CRP with the total flux in all open channels of the arrangement b in the valley a and using Eq. (85b), we have

$$\theta(R_b-R_a)N_{ab}(E) = i\sum_{n_b}^{\text{open}} \langle \psi_{n_b}|F_b(R_b)G(E)F_a(R_a)|\psi_{n_b}\rangle. \tag{89}$$

Adding Eqs. (88) and (89) and taking into account Eq. (76), we obtain

$$N_{ab}(E) = 2\pi i\ \text{tr}[F_b(R_b)G(E)F_a(R_a)\delta(H-E)]. \tag{90}$$

As follows from Eq. (86),

$$\text{tr}[F_b(R_b)G(E)F_a(R_a)G(E)] = 0, \tag{91}$$

thus Eq. (90) can be cast in the form

$$N_{ab}(E) = -\text{tr}[F_b(R_b)G(E)F_a(R_a)G^*(E)]. \tag{92}$$

This coincides with formula (7) except for the sign. This apparent difference is explained by the fact that both flux operators in Eq. (7) were assumed to be defined democratically with respect to the direction of the reaction path, as was the case for the one-dimensional model discussed in Sec. II. For the present case the reaction path goes from a through I to b or vice versa, and the operators $F_a(R_a)$ and $F_b(R_b)$ represent fluxes going in the different directions. Formulas (90) and (92) generalize Eqs. (36) and (38). The counterparts of Eqs. (39) and (40) can also be obtained for the present case; however, we shall not discuss them here.

In coordinate representation Eq. (92) reads

$$\begin{aligned} N_{ab}(E) = \frac{1}{4}\int_{\mathcal{S}_a} d\Omega_a \int_{\mathcal{S}_b} d\Omega_b \\ \times\Bigg[&\frac{\partial G(\mathbf{R}_a,\mathbf{R}_b;E)}{\partial R_a}\frac{\partial G^*(\mathbf{R}_a,\mathbf{R}_b;E)}{\partial R_b} \\ &+ \frac{\partial G^*(\mathbf{R}_a,\mathbf{R}_b;E)}{\partial R_a}\frac{\partial G(\mathbf{R_a},\mathbf{R}_b;E)}{\partial R_b} \\ &- G(\mathbf{R}_a,\mathbf{R}_b;E)\frac{\partial^2 G^*(\mathbf{R}_a,\mathbf{R}_b;E)}{\partial R_a \partial R_b} \\ &- G^*(\mathbf{R}_a,\mathbf{R}_b;E)\frac{\partial^2 G(\mathbf{R}_a,\mathbf{R}_b;E)}{\partial R_a \partial R_b}\Bigg]. \end{aligned} \tag{93}$$

This equation specifies the meaning of formula (7) within the hyperspherical formulation. Here R_a and R_b are arbitrary but not smaller than R_m. Letting both R_a and R_b go to ∞ and using the boundary conditions (75), from Eq. (93) we obtain

$$\begin{aligned} N_{ab}(E) = \sum_{n_a,n_b}^{\text{open}} k_{n_a}(R_a)k_{n_b}(R_b) \\ \times |G_{n_a n_b}(R_a,R_b;E)|^2|_{R_a,R_b\to\infty}, \end{aligned} \tag{94}$$

where

$$k_n(R) = \sqrt{2[E-U_n(R)]} \tag{95}$$

and

$$G_{nn'}(R,R';E)=\int_{\mathcal{S}} d\Omega \int_{\mathcal{S}} d\Omega' G(\mathbf{R},\mathbf{R}';E) \times \Phi_n(\Omega;R)\Phi_{n'}(\Omega';R'). \quad (96)$$

Equations (94)–(96) specify the meaning of Eq. (10). In order to minimize the region where the Green's function is to be constructed, in the following we put in Eq. (94) $R_a=R_b=R_m$ (which restores the original definition of $\mathcal{S}_a$ and $\mathcal{S}_b$). Assuming R_m to be large but finite amounts to using semiclassical approximation to the outgoing wave boundary conditions (75), which makes our approach practical. It is worth noting that the possibility to use different radii R_a and R_b in Eq. (93) is a manifestation of a larger flexibility of this formula. Indeed, basing on the flux conservation the hyperspherical segments $\mathcal{S}_a$ and $\mathcal{S}_b$ in Eq. (93) can be replaced by more general boundary surfaces between the reaction zone I and the arrangements a and b; however, we do not detail this issue here.

Let us introduce a diagonal matrix $\mathbf{k}(R)$ with elements (95) and a symmetric matrix $\mathbf{G}(R,R';E)$ with elements (96). If both R and R' are larger than R_m, then these matrices can be partitioned into blocks similarly to Eq. (2):

$$\mathbf{k}(R)=\begin{pmatrix} \mathbf{k}_a(R) & \mathbf{0} \\ \mathbf{0} & \mathbf{k}_b(R) \end{pmatrix} \quad (97)$$

and

$$\mathbf{G}(R,R';E)=\begin{pmatrix} \mathbf{G}_{aa}(R,R';E) & \mathbf{G}_{ab}(R,R';E) \\ \mathbf{G}_{ba}(R,R';E) & \mathbf{G}_{bb}(R,R';E) \end{pmatrix}. \quad (98)$$

Let us introduce a matrix

$$\mathbf{P}_{ab}(R_m;E)=\sqrt{\mathbf{k}_a(R_m)}\,\mathbf{G}_{ab}(R_m,R_m;E)\,\sqrt{\mathbf{k}_b(R_m)}. \quad (99)$$

Then Eq. (94) can be presented in the form

$$N_{ab}(E)=\mathrm{tr}[\mathbf{P}_{ab}(R_m;E)\mathbf{P}^{\dagger}_{ab}(R_m;E)]|_{R_m\to\infty}. \quad (100)$$

Comparing this with Eq. (3) and noting that both equations should give identical results for a continuous interval of E, we obtain

$$|S_{n_a n_b}(E)|^2=|P_{n_a n_b}(R_m;E)|^2|_{R_m\to\infty}. \quad (101)$$

We remark that this formula can be derived more rigorously. Thus, in principle, knowing the matrix (99) one can calculate all the state-to-state reaction probabilities. However the convergence as R_m grows in this case is not as fast as for the CRP, and we shall not discuss such calculations in this paper.

C. Reaction eigenprobabilities

Let us return to Eq. (3) and consider the matrix $\mathbf{S}_{ab}(E)\mathbf{S}^{\dagger}_{ab}(E)$. This matrix has the dimension $\overline{n_a}$ equal to the number of open channels in the arrangement a. It is Hermitian, so it can be diagonalized by a unitary transformation of the asymptotic states in the arrangement a and its eigenvalues $p^a_n(E)$ are real. Moreover, they lie in the interval $0\leqslant p^a_n(E)\leqslant 1$, where the first inequality follows from the nonnegativeness of all diagonal elements of the considered matrix, and the second one results from the unitarity of the scattering matrix (2). We can invert the order of the two matrices under the symbol of trace in Eq. (3) without changing the value of the expression and consider the matrix $\mathbf{S}^{\dagger}_{ab}(E)\mathbf{S}_{ab}(E)=(\mathbf{S}_{ba}(E)\mathbf{S}^{\dagger}_{ba}(E))^*$. Its dimension $\overline{n_b}$ is equal to the number of open channels in the arrangement b and, for the same reasons, its eigenvalues $p^b_n(E)$ are real and satisfy $0\leqslant p^b_n(E)\leqslant 1$. In fact, it can be shown that the two sets $p^a_n(E)$, $n=1,\ldots,\overline{n_a}$, and $p^b_n(E)$, $n=1,\ldots,\overline{n_b}$, actually coincide, except that the longer one contains additional $|\overline{n_a}-\overline{n_b}|$ zero eigenvalues [35]. Thus we can omit the superscripts a and b and rewrite Eq. (3) as follows

$$N_{ab}(E)=\sum_{n}^{\overline{n}} p_n(E), \quad (102)$$

where $\overline{n}=\min(\overline{n_a},\overline{n_b})$. The eigenvalues $p_n(E)$, called reaction eigenprobabilities, were first considered in Ref. [12]. They can be compared with the eigenphase shifts [1] whose sum is defined by Eq. (1). The above discussion defines $p_n(E)$ in terms of the scattering matrix. Comparing Eqs. (100) and (102), the reaction eigenprobabilities can be expressed in terms of the Green's function as eigenvalues of the matrix $\mathbf{P}_{ab}(R_m;E)\mathbf{P}^{\dagger}_{ab}(R_m;E)$ for sufficiently large R_m. This explains how $p_n(E)$ can be calculated in the present approach.

D. Construction of the Green's function

To implement the above equations one has to construct the Green's function $G(\mathbf{R},\mathbf{R}';E)$ with its two arguments lying in the valleys a and b. This could be done by expanding it in terms of some global basis spanning the whole reaction zone I which would lead to an algebraic equation similar to Eq. (49). However, in multidimensional case the size of the basis required may be too large. For example, for triatomic systems it should be similar to that used in absorbing potential calculations [11–16], although in our approach we could expect a reduction by about a factor of three due to the reduction of the size of the reaction zone to be considered, as was demonstrated for the one-dimensional case in Ref. [19] and Sec. II B. Tackling large matrices is a difficult problem in the spirit of quantum chemistry calculations, and we shall not discuss such a global approach here. Instead, we describe a method which is practical and falls most naturally in the framework of hyperspherical approach as well as many other quantum scattering technologies. The idea is to divide the reaction zone I into a number of smaller regions, so that each of them can be spanned by a basis of moderate size, and then to match different pieces with each other thus obtaining a global solution. This idea can be easily implemented in hyperspherical geometry by using the $\mathcal{R}$-matrix method.

Let us introduce an $\mathcal{R}$-operator,

$$\psi(R,\Omega)=\int_{\mathcal{S}}\mathcal{R}(\Omega,\Omega';R)\frac{\partial\psi(R,\Omega')}{\partial R}d\Omega', \qquad (103)$$

where $\psi(\mathbf{R})$ is an arbitrary solution of Eq. (57) satisfying the boundary condition (65). For any R, the kernel $\mathcal{R}(\Omega,\Omega';R)$ here can be expanded in terms of the HSA channel functions. The coefficients in this expansion are defined by

$$\mathcal{R}_{nn'}(R)=\int_{\mathcal{S}}d\Omega\int_{\mathcal{S}}d\Omega'\mathcal{R}(\Omega,\Omega';R)\Phi_n(\Omega;R)\Phi_{n'}(\Omega';R), \qquad (104)$$

and constitute the $\mathcal{R}$ matrix. Methods of calculating this matrix are very well developed [29]. Let $\mathcal{R}_{nn'}(R_m)$ be the $\mathcal{R}$ matrix at $R=R_m$, i.e., on the outer boundary of the reaction zone I. Let us write down the Green's formula (84) in coordinate representation:

$$\psi(\mathbf{R})=\frac{1}{2}\int_{\mathcal{S}}\left(G(\mathbf{R},\mathbf{R}';E)\frac{\partial\psi(\mathbf{R}')}{\partial R'}-\frac{\partial G(\mathbf{R},\mathbf{R}';E)}{\partial R'}\psi(\mathbf{R}')\right)d\Omega', \quad R<R'. \qquad (105)$$

Putting here $R=R'=R_m$, comparing with Eq. (103), and using the boundary conditions (75) and definitions (96) and (104), we obtain

$$\mathbf{G}(R_m,R_m;E)=2\mathcal{R}(R_m)[\mathbf{I}-i\mathbf{k}(R_m)\mathcal{R}(R_m)]^{-1}. \qquad (106)$$

This equation specifies the meaning of Eq. (11) within the hyperspherical formulation and provides a practical recipe to implement our approach.

IV. ILLUSTRATIVE CALCULATIONS

As has been mentioned above, our method was illustrated in Ref. [20] by application to muon transfer reaction in $dt\mu$. In this section, we discuss two computationally more challenging applications of the method to atom-diatom chemical reactions. Recently, two of us have developed a new very efficient and accurate quantum scattering code for calculating collisions in heavy-light-heavy (HLH) triatomic systems [36]. This code was used for clarifying mechanisms of light atom transfer reactions in several HLH systems [37,38]. Here, we show that Eqs. (94) and (106) can be easily implemented on the basis of this code and that using these equations one can essentially reduce the size of the region to be considered for calculating the CRP as compared to that which is essential for calculating the scattering matrix.

A. Computational procedure

Let us outline briefly a general scheme of the present computational procedure; for more details we refer to [36]. Consider a system of three atoms A, B, and C, and let $a=A+CB$ and $b=B+CA$, so the results of the previous section will be applied to transfer of the atom C between atoms A and B. To comply with convention adopted in hyperspherical calculations of chemical reactions and with notation used in Ref. [36] we introduce a new hyperradial variable,

$$R=\rho\left(\frac{m_Am_Bm_C}{m_{\rm tot}}\right)^{1/4}, \qquad (107)$$

where R is defined by Eq. (53), m_A, m_B, and m_C are the masses of the atoms, and $m_{\rm tot}=m_A+m_B+m_C$ is the total mass of the system. Configuration space of the system is parametrized by the hyperradius ρ and two hyperangular variables ξ and η called hyperspherical elliptic coordinates [39] which are used as coordinates on hypersphere $\mathcal{S}$. For HLH systems (C is assumed to be the light atom), the variables ξ and η approximately correspond to the vibrational and rotational degrees of freedom, respectively. Taking advantage of this circumstance greatly facilitates numerical solution of the HSA eigenvalue problem (61). Solving Eq. (61) yields a set of HSA channel functions $\Phi_n(\xi,\eta;\rho)$, $n=1,\ldots,N_{\rm ch}$, which for any ρ satisfy

$$\int_{2\gamma}^{2\pi-2\gamma}d\xi\int_{-2\gamma}^{2\gamma}d\eta(\cos\eta-\cos\xi)\Phi_n(\xi,\eta;\rho)\Phi_m(\xi,\eta;\rho)=\delta_{nm}, \qquad (108)$$

where

$$\tan\gamma=\sqrt{\frac{m_Cm_{\rm tot}}{m_Am_B}}, \quad 0\leqslant\gamma\leqslant\frac{\pi}{2}. \qquad (109)$$

The Schrödinger equation (57) is considered in a finite interval $\rho\in[\rho_0,\rho_m]$. Here ρ_0 is the radius of the hard core region where wave function is assumed to vanish, see Eq. (65), and ρ_m is the matching radius. This interval is divided into a number of sectors. In each sector, a Hermitized version of Eq. (57) corresponding to imposing the $\mathcal{R}$-matrix boundary conditions is solved. This is done using the slow/smooth variable discretization method [40]: the dependence of the solutions on hyperradius ρ is expanded in terms of a set of DVR basis functions defined within the sector, and their dependence on hyperangular variables (ξ,η) is represented by the HSA channel functions taken at the corresponding set of hyperradial quadrature points. This yields the $\mathcal{R}$-matrix basis for the sector. Constructing such basis for each sector completes the energy independent part of the calculations. Thus obtained information permits one to consider scattering in a wide energy range whose upper boundary is the higher the larger is the number $N_{\rm ch}$ of HSA channels included in the calculation. For any energy E in this range, the $\mathcal{R}$ matrix can be propagated between boundaries of sectors using the technique of Ref. [41]. Starting from $\rho=\rho_0$ with the initial condition $\mathcal{R}(\rho_0)=0$ we obtain the $\mathcal{R}$ matrix at the matching surface, $\mathcal{R}(\rho_m)$. Then we can extract the scattering matrix $\mathbf{S}(E)$ by applying a two-dimensional matching procedure described in Ref. [36] and calculate the CRP $N_{ab}(E)$ from Eq. (3). This procedure was used for calculating the CRP in Refs. [36–38] and we shall refer to it as the scattering

method. Alternatively, the CRP can be calculated using Eqs. (94) and (106), which will be referred to as the direct method.

In both direct and scattering calculations reported below we shall use the same numbers of HSA channels $N_{\rm ch}$ and the same values of the hard core radius ρ_0, the only difference in the calculational parameters being in the value of the matching radius ρ_m. The convergence of individual elements of scattering matrix with respect to ρ_m is much slower than that of the CRP as was demonstrated in [20] (see Fig. 3 therein). Here we shall not discuss this issue again; all the scattering results presented below are obtained from converged scattering matrix. An important issue in the following discussion is to demonstrate convergence of the direct results for $N_{ab}(E)$ as the matching radius ρ_m grows. In Ref. [20], this convergence was characterized by the potential ridge function $U_r(\rho)$. The concept of potential ridge is well familiar from hyperspherical analysis of collinear reactions [42] and recently it has been generalized to light atom transfer reactions in HLH systems in three dimensions [37,38] on the basis of the approach developed in Ref. [36]. The results of Refs. [37,38] suggest that for a given energy E reaction does not occur at $\rho>\rho_r$, where ρ_r is defined by $E=U_r(\rho_r)$. So for calculating the CRP at this energy it should be sufficient to consider the region $\rho<\rho_r$. In this paper instead of the potential ridge we consider the function

$$w_{N_{\rm ch}}(\eta;\rho)=\sum_{n=1}^{N_{\rm ch}}\int_{2\gamma}^{2\pi-2\gamma}\Phi_n^2(\xi,\eta;\rho)(\cos\eta-\cos\xi)d\xi \tag{110}$$

which has a meaning of the cumulative density of the HSA channels included in the calculation projected on the η coordinate. As follows from Eq. (108), this function satisfies

$$\int_{-2\gamma}^{2\gamma} w_{N_{\rm ch}}(\eta;\rho)d\eta=N_{\rm ch}. \tag{111}$$

As ρ grows, the regions occupied by the arrangements a and b localize on hypersphere near the points $(\xi,\eta)=(2\gamma, -2\gamma)$ and $(2\gamma,2\gamma)$, respectively, hence at large ρ function (110) splits into two disconnected parts located near $\eta=\pm 2\gamma$. These parts are separated by a potential barrier whose top considered as a function of ρ approximately coincides with $U_r(\rho)$. The larger is the number of channels $N_{\rm ch}$ included in Eq. (110), the farther in ρ the separation occurs. Thus the projected density (110) illustrates another facet of the potential ridge as a barrier separating arrangements.

B. Examples

As the first example we consider the reaction

$$O(^3P)+HCl\leftrightarrow OH+Cl \tag{112}$$

for two different PESs: one is the LEPS PES with the parameters defined in Ref. [43], and the other is a more elaborate fit to *ab initio* calculations proposed in Ref. [44], which we shall refer to as KSG. For this system $A=O$, $B=Cl$, $C=H$, $R\approx 77.57\rho$, and $\gamma\approx 0.30$. We use atomic units for ρ and the energy E will be measured in eV from the ground state of HCl. Reaction (112) is almost isoergic: the ground state of OH lies higher than that of HCl by only 0.040 eV which defines the energetic threshold. The classical threshold is defined by the position of the transition state which lies at 0.168 eV for the LEPS PES. In the present calculations we use the same number of HSA channels $N_{\rm ch}=100$ and the same values of the hard core radius $\rho_0=6.5$ for the LEPS and $\rho_0=4.9$ for the KSG PES as were used in Ref. [36].

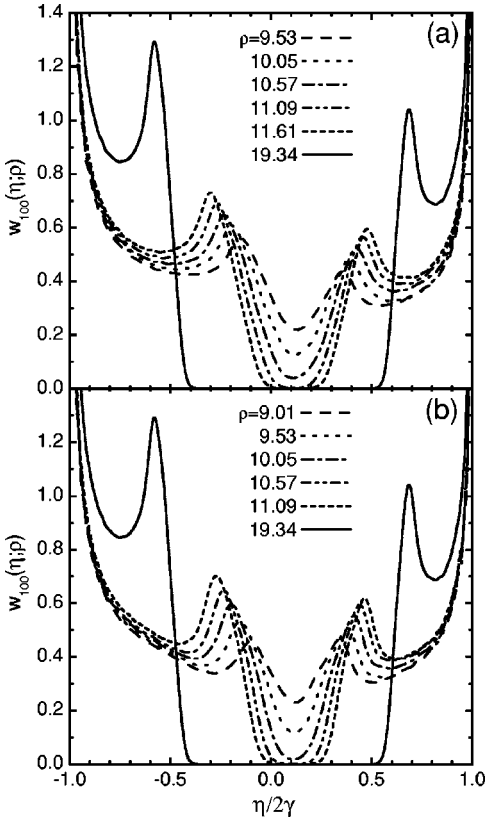

FIG. 2. Projected density function (110) for O–Cl–H calculated for the LEPS (a) and KSG (b) PESs with $N_{\rm ch}=100$ HSA channels for several representative values of ρ. The arrangements $O(^3P)+HCl$ and $OH+Cl$ are located in the left and in the right parts of the figures, respectively. These figures illustrate separation of the arrangements along the η coordinate as ρ grows.

Figures 2 show projected density (110) for the two PESs calculated for several representative values of ρ. Note that apart from a slight shift in ρ between the corresponding curves these figures look quite similar, although the HSA potentials defined by Eq. (61) considerably differ for these two PESs, as can be seen from Fig. 9 in Ref. [36]. The central minimum of the function (110) in Fig. 2 indicates the position of the potential barrier separating the arrangements $O(^3P)+HCl$ on the left and $OH+Cl$ on the right, while the two adjoined maxima indicate the regions where reflection from this barrier in the motion along the η coordinate takes place. As was mentioned above, at large ρ the function (110) splits into two disconnected parts localized near $\eta=\pm 2\gamma$. The value of $\rho=\rho_s$ where this splitting occurs depends on $N_{\rm ch}$. As can be seen from the figures, for the present case $\rho_s\approx 11$ for the LEPS and $\rho_s\approx 10.3$ for the KSG PES. At ρ

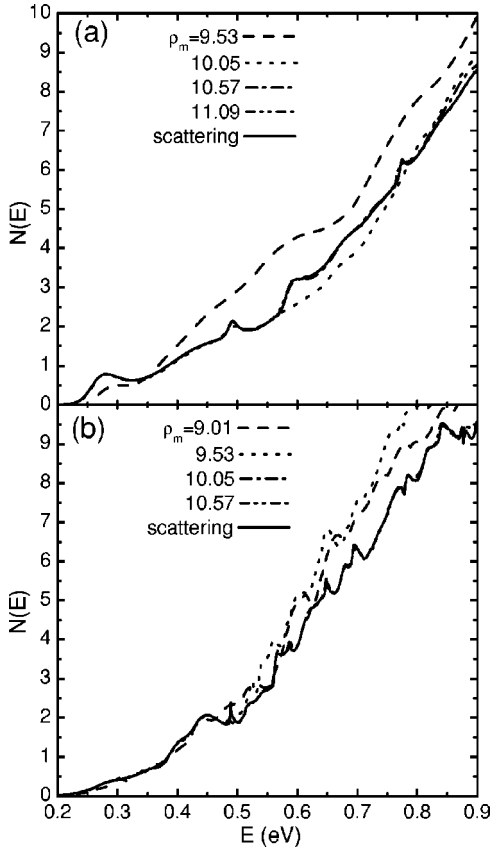

FIG. 3. Convergence of the direct results for the CRP of reaction (112) calculated by Eqs. (94) and (106) using the LEPS (a) and KSG (b) PESs. The values of ρ_m used in the calculations coincide with that shown in Figs. 2. The solid curves are the scattering results taken from [36] calculated by Eq. (3). Those of the broken curves which are not seen cannot be distinguished by the eye from the solid curves in the scale of the figures.

$>\rho_s$ reaction can proceed only via tunneling, so it is suppressed. Hence one could expect that Eqs. (94) and (106) yield converged results for the CRP if $\rho_m > \rho_s$. The values of ρ shown in the figures are equidistant and lie in the vicinity of $\rho=\rho_s$, except the largest ρ which coincides with the value of the matching radius ρ_m used in the scattering calculations [36]. At this ρ there is a wide gap along the η coordinate between the two parts of the function (110), so the arrangements are completely separated.

Figure 3 show present direct results for reaction (112) calculated with the same values of the matching radius ρ_m as shown in Fig. 2. The solid curves in these figures present results obtained by the scattering method [36]. These figures confirm the above expectation that the direct results for the CRP rapidly converge as ρ_m becomes larger than ρ_s. In fact, they converge even earlier: for the LEPS PES [Fig. 3(a)] the direct results become almost indistinguishable by the eye from the scattering results already for $\rho_m \approx 10.6$, and for the KSG PES [Fig. 3(b)] this happens for $\rho_m \approx 10$. Thus using Eqs. (94) and (106) the CRP for reaction (112) can be calculated by considering an interval of ρ about three times smaller than that which has been considered in [36] for obtaining accurate results for the scattering matrix.

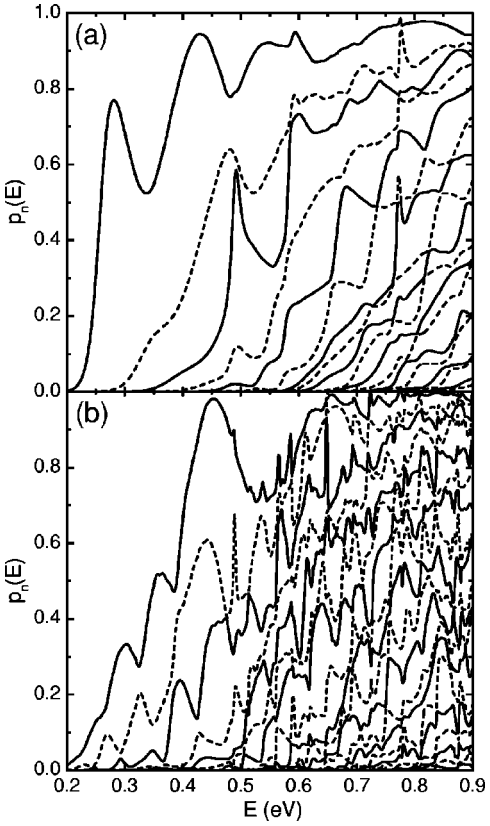

FIG. 4. Present converged results for the eigenprobabilities of reaction (112) calculated for the LEPS (a) and KSG (b) PESs. In both cases 18 functions $p_n(E)$ are shown. To reveal avoided crossings between different curves, the functions $p_n(E)$ with odd (even) numbers are plotted by solid (dashed) lines.

Figure 4 show present converged results for the eigenprobabilities of reaction (112). For both LEPS and KSG PESs only 18 lowest functions $p_n(E)$ are shown; the higher reaction eigenprobabilities have negligible values in the considered interval of E. Careful analysis of the figures shows that peaks of the CRP seen in Fig. 3 are caused by rapid variation of individual terms in the sum (102). Moreover, at the energies where such peaks occur there are avoided crossings between functions $p_n(E)$ with different n, as can be seen from Fig. 4. These features suggest that peaks of the CRP can be associated with some kind of ''transition state resonances,'' probably of the type considered in Ref. [45], although to confirm this interpretation an analysis of the corresponding wave function is needed. From Fig. 4 it is clear that functions $p_n(E)$ provide a very valuable information about reaction dynamics and worth to be studied in more detail. In particular, these figures reveal a huge difference between the two considered PESs describing reaction (112).

As the second example we consider the exo/endo-ergic reaction

$$\mathrm{Br}+\mathrm{HCl}\leftrightarrow\mathrm{BrH}+\mathrm{Cl} \tag{113}$$

for the LEPS PES with the parameters defined in Ref. [46]. For this system we have: $A=\mathrm{Br}$, $B=\mathrm{Cl}$, $C=\mathrm{H}$, $R\approx 95.03\rho$, and $\gamma\approx 0.20$. The energy E will be measured again from the

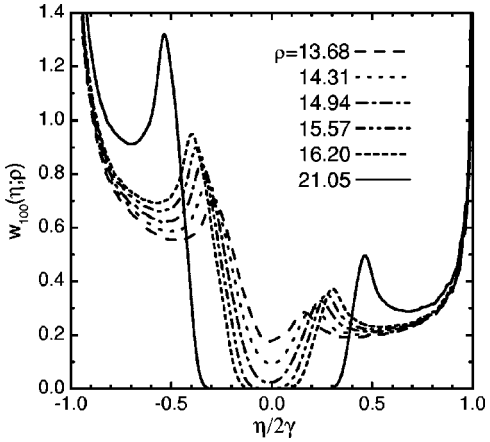

FIG. 5. Same as in Fig. 2, but for Br–Cl–H. The arrangements Br+HCl and BrH+Cl are located in the left and in the right parts of the figure, respectively.

ground state of HCl. Then the ground state of BrH lies at 0.68 eV which defines the energetic threshold. Scattering calculations for this reaction by the method developed in Ref. [36] were reported in Ref. [38]. In the present calculations we use the same number of HSA channels $N_{\mathrm{ch}}=100$ and the same value of the hard core radius $\rho_0=8$ as were used in Ref. [38]. Figures 5–7 present results similar to that shown in Figs. 2–4 for the previous system. The arrangements Br+HCl and BrH+Cl are located in the left and in the right parts of Fig. 5, respectively. Of the 100 HSA channels included in Eq. (110) in the present case 74 belong to the former and only 26 to the latter arrangement at $\rho\rightarrow\infty$, so the left wings of the projected densities shown in Fig. 5 are about three times higher than the right ones. For this system separation of the arrangements along the η coordinate occurs at $\rho_s\approx 15.3$. The largest value of ρ shown in Fig. 5 coincides with the matching radius ρ_m used in the scattering calculations [38]. Figure 6 demonstrates convergence of the direct results for the CRP calculated for the same values of ρ_m as shown in Fig. 5. As can be seen from this figure, the direct

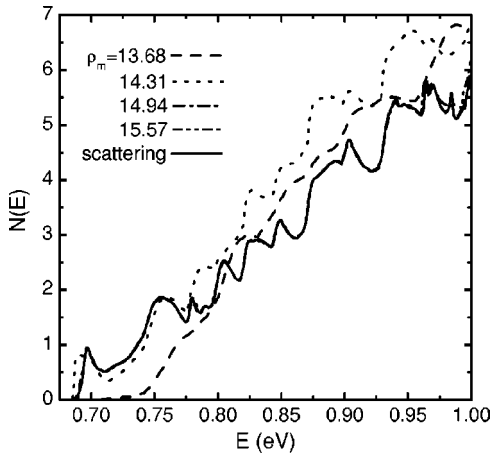

FIG. 6. Same as in Fig. 3, but for reaction (113). The values of ρ_m used in the calculations coincide with that shown in Fig. 5. The solid curves are the scattering results taken from [38].

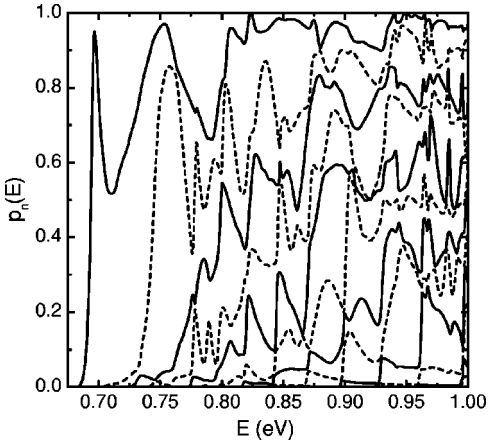

FIG. 7. Same as in Fig. 4, but for reaction (113). Here 11 eigenprobabilities $p_n(E)$ are shown.

results obtained with $\rho_m\approx 15$ practically coincide with the accurate scattering results of Ref. [38]. This means that in calculating the CRP of reaction (113) Eqs. (94) and (106) permit one to reduce the interval of ρ by a factor of two as compared to that considered in Ref. [38]. Finally, Fig. 7 shows present converged results for the eigenprobabilities of reaction (113). Only 10 functions $p_n(E)$ are shown in the figure. Similarly to Fig. 4, one can see that there is a lot of avoided crossings and peaks corresponding to resonance peaks of the CRP seen in Fig. 6. To clarify the nature of these features, however, goes beyond the scope of this paper.

V. SUMMARY

In this paper we have presented a complete development of the recently proposed [20] new approach to the theory of CRP and provided additional demonstrations of its numerical efficiency. Our main formula (7) and its implementation in terms of the Wigner-Eisenbud $\mathcal{R}$ matrix given by Eqs. (10) and (11) rest on solid grounds of standard scattering theory and are free from the difficulties and ambiguities of previous formulations. These formulas enable one to calculate the CRP and reaction eigenprobabilities directly and with a considerable reduction of the computational labor as compared to that required for calculating the scattering matrix, at least using the techniques employed by our group. Here we have demonstrated the implementation of our approach in the framework of hyperspherical method on the basis of the program for calculating light atom transfer reactions in heavy-light-heavy systems developed in Ref. [36]. However, Eqs. (10) and (11) can be easily implemented on the basis of any other quantum scattering code which uses the $\mathcal{R}$-matrix method; see Ref. [29]. Upgrading such code in this way would make it capable of calculating the CRP even in situations where the calculation of scattering matrix is not feasible.

ACKNOWLEDGMENTS

This work was partially supported by a Grant-in-Aid for Scientific Research on Priority Area ''Molecular Physical

Chemistry'' and a Research Grant No. 10441079 from The Ministry of Education, Science, Culture, and Sports of Japan. O.I.T. gratefully acknowledges partial support from the INTAS under Grant No. 97-11032 ''Theoretical Study of Exotic Atomic and Molecular Systems.''

APPENDIX: TRANSMISSION PROBABILITY OF ONE-DIMENSIONAL SYMMETRIC POTENTIAL BARRIERS FROM SIEGERT PSEUDOSTATE EIGENVALUES

As was first realized in Ref. [3] and discussed in detail in this paper, the CRP can be expressed in terms of the outgoing wave Green's function. On the other hand, it is well known [1,47] that under rather general conditions the Green's function can be expanded in terms of Siegert states which are solutions to the Schrödinger equation satisfying outgoing wave boundary conditions [48]. So, there must be a way to express the CRP in terms of the Siegert states. This idea is not new and it has been already discussed in literature [30,49]. Its implementation apart from bringing conceptual consistency and beauty to the formulation promises also certain computational advantages. The point is that Siegert states do not depend on energy, so having constructed a set of Siegert states, which might be a difficult task but which must be done only once, one should be able to calculate the CRP in a wide energy range. The center of gravity of calculations in this approach is thus shifted to constructing the Siegert states.

Recently, we have proposed an efficient method for calculating Siegert *pseudo*states (SPS) defined as solutions to the Schrödinger equation satisfying outgoing wave boundary conditions imposed at a *finite* point [27]. In Ref. [28], we have shown that for the one-channel scattering problem bound, antibound, and resonance states are represented by individual SPS and derived SPS expansions for continuous energy wave function, Green's function, and scattering matrix, i.e., for all the important objects of the theory. So far this formulation is developed only for scattering described by a single radial equation, but it can be easily extended to scattering by one-dimensional potentials considered on the whole axis if the potential function is symmetric. Here we show how in this case one can calculate the CRP knowing only the SPS eigenvalues.

For the one-dimensional scattering problem discussed in Sec. II A, the SPSs are defined by:

$$[H(x)-E]\phi(x)=0, \tag{A1a}$$

$$\left(\frac{d}{dx}+k(x)\right)\phi(x)\bigg|_{x=-x_m}=0, \tag{A1b}$$

$$\left(\frac{d}{dx}-k(x)\right)\phi(x)\bigg|_{x=x_m}=0, \tag{A1c}$$

where $H(x)$ and $k(x)$ are given by Eqs. (13) and (43), x_m is the cutoff radius, and we again use semiclassical version of the outgoing wave boundary conditions. Equations (A1) can be satisfied only for a discrete set of generally complex energies $E=E_n$, so we are dealing with an eigenvalue problem. For symmetric potentials, $V(x)=V(-x)$, the eigenfunctions of Eqs. (A1) are either even or odd. The even and odd SPSs will be considered separately and all the corresponding quantities will be indicated by $+$ and $-$ superscript, respectively. The following discussion is equally applicable to both cases, so we shall omit this superscript for a while until the final result will be presented. Similarly to Sec. II B, we introduce a basis $\pi_i(x)$, $i=1,\ldots,N$, which is orthonormal in the interval $[-x_m,x_m]$ and becomes complete in the limit $N\to\infty$. The SPS eigenfunctions $\phi(x)$ can be expanded in terms of this basis:

$$\phi(x)=\sum_{j=1}^{N} c_i\pi_i(x), \quad -x_m\leqslant x\leqslant x_m. \tag{A2}$$

Substituting this expansion into Eq. (A1a) and using the boundary conditions (A1b) and (A1c), for the vector c of coefficient c_i one obtains

$$(\mathbf{A}+\lambda\mathbf{B}+\lambda^2\mathbf{I})c=0, \tag{A3}$$

where

$$\lambda=i\sqrt{2[E-V(x_m)]}, \tag{A4}$$

$$\mathbf{A}=2[\tilde{\mathbf{H}}-V(x_m)\mathbf{I}], \tag{A5}$$

$$\mathbf{B}=-2\mathbf{L}(x_m), \tag{A6}$$

and the matrices $\tilde{\mathbf{H}}$ and $\mathbf{L}(x)$ are defined by Eqs. (50) and (51). The methods of solving quadratic algebraic eigenvalue problem (A3) and the properties of its solutions are discussed in Ref. [28]. This equation can be reduced to a linear eigenvalue problem of doubled dimension $2N$ which yields $2N$ eigenpairs λ_n and $c^{(n)}$ defining $2N$ SPSs. Having the SPSs, one can construct the Green's function and then calculate the CRP by Eq. (42). We skip the derivation which is quite similar to that of Ref. [28] and is based on Eq. (44) therein. The final result for the CRP reads:

$$N_{ab}(E)=\frac{1}{4}\left|\prod_{n=1}^{2N^+}\frac{\lambda_n^+ +\lambda}{\lambda_n^+ -\lambda}-\prod_{n=1}^{2N^-}\frac{\lambda_n^- +\lambda}{\lambda_n^- -\lambda}\right|^2, \tag{A7}$$

where λ is related to E by Eq. (A4), and $\lambda_n^{\pm}$ are eigenvalues of Eq. (A3) related to the corresponding SPS energy eigenvalues $E_n^{\pm}$ by the same equation. This formula expresses $N_{ab}(E)$ in terms of the SPS eigenvalues defined for the given cutoff radius x_m and the numbers of basis functions $N^{\pm}$. A converged result will be obtained as these parameters increase.

We illustrate this method by the same two examples as were considered in Ref. [19]. In the calculations reported below, we use even and odd Legendre polynomials as bases for even and odd SPSs, respectively. Then matrix $\mathbf{L}(x_m)$ and the kinetic part of $\tilde{\mathbf{H}}$ can be calculated analytically, while matrix elements of the potential $V(x)$ were calculated using

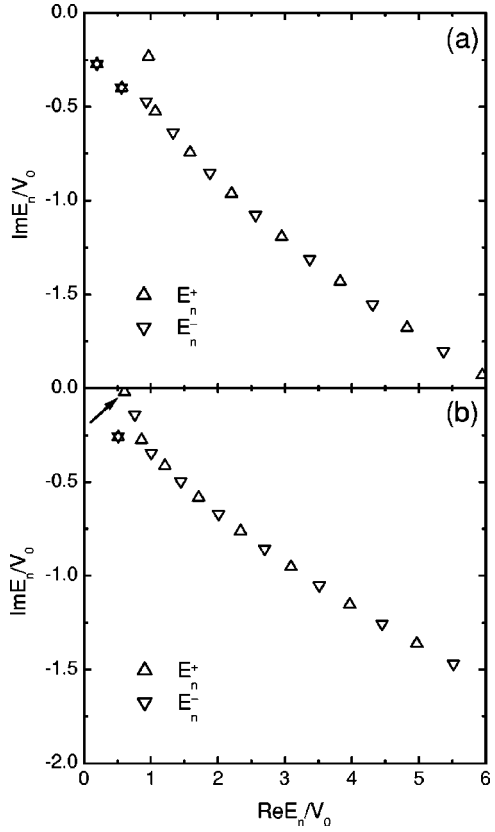

FIG. 8. Triangles (inverted triangles)—even (odd) SPS energy eigenvalues E_n^+ (E_n^-) (a) for the Eckart potential (A8) and (b) for the double maximum potential (A9). The eigenvalues were obtained by solving Eq. (A3) and then converting from λ to E using Eq. (A4). The results were obtained with $x_m=3d$ and $N^{\pm}=50$. All the eigenvalues shown are converged with respect to $N^{\pm}$. The arrow indicates the only SPS eigenvalue that converges as x_m grows, which represents the resonance state supported by the potential (A9).

Gauss-Legendre quadrature with the number of points equal to the number of polynomials, i.e., in the spirit of a DVR.

The first example is the Eckart potential,

$$V(x)=V_0\,\mathrm{sech}^2(x/d), \quad d=a\sqrt{m}, \tag{A8}$$

with the parameters $V_0=0.0156$ a.u., $a=0.734$ a.u., and $m=1061$ a.u. [30] (we recall that our x is a mass-scaled coordinate). Figure 8(a) shows a part of the distribution of the SPS energy eigenvalues obtained by solving Eq. (A3) for some particular values of x_m and $N^{\pm}$. The eigenvalues are distributed symmetrically with respect to the real axis (complex eigenvalues occur in complex conjugate pairs), so only the lower half of the complex energy plane is shown. All the eigenvalues shown in the figure are converged with respect to $N^{\pm}$, but none of them converges as x_m grows (for more details on this behavior see Ref. [28]). Most of the SPS eigenvalues are the cutoff poles corresponding to a kind of ''particle-in-a-box'' states [28] and fall along a parabola-like branch whose asymptotic behavior at large n is discussed in Ref. [28]. These eigenvalues have nothing to do with the true Siegert energy eigenvalues for the Eckart potential discussed in Ref. [49]. Only the one that lies out of line and whose dependence on x_m is different from that for other eigenvalues is a remnant of a true Siegert pole. However, in spite of the fact that the SPS eigenvalues depend on x_m, the CRP given by Eq. (A7) rapidly converges as x_m grows. We have analyzed this convergence for the same energy $E=0.0118$ a.u. as was considered in Ref. [19]. Our results are virtually identical to that shown in Fig. 2 of Ref. [19]: a relative error decreases oscillatorily as x_m grows, and for $x_m>2d$ it is less than ± 0.5 %. More generally, formula (A7) yields a relative error less than ± 0.5 % for all energies $E\geqslant 0.1V_0$ using the SPS eigenvalues calculated with $x_m=4d$ and $N^{\pm}=15$.

The second example is a symmetric double maximum barrier,

$$V(x)=V_0[1/2+(x/d)^2]\mathrm{sech}^2(x/d), \tag{A9}$$

with the same values of the parameters as above. Figure 8(b) shows a distribution of the SPS energy eigenvalues for this potential. In this case the situation is slightly different: there is one eigenvalue that rapidly converges as x_m grows. This eigenvalue is indicated by the arrow in Fig. 8(b) and corresponds to a true resonance state supported by the potential. The converged value of the resonance energy is $E/V_0=0.604\,841\,555-0.020\,516\,3790i$ with an error of ± 1 in the last digit quoted (this was obtained for V_0 cited above and $1/d=0.041826$ a.u. exactly). The ratio $\mathrm{Im}\,E/\mathrm{Re}\,E$ for our result is about three times larger than that for the resonance energy reported in Ref. [19]. However, the SPS method was shown to yield a very high precision in calculating resonances [27,28,50], so we believe that our result is more accurate. This resonance causes a sharp peak in the function $N_{ab}(E)$ (see Fig. 5 in Ref. [19]). The ability to unambiguously associate such peaks in the energy dependence of CRP with individual resonance states of the system is another advantage of the present approach. Finally, the rate of convergence of our results for $N_{ab}(E)$ obtained from Eq. (A7) as x_m grows fully agrees with that demonstrated in Ref. [19].

Thus in the considered one-dimensional case the SPS approach to the theory of CRP resulting in formula (A7) is very efficient and accurate. Whether this approach can be extended to a multi-dimensional case remains an open problem which is doubtlessly worth pursuing.

[1] R. G. Newton, *Scattering Theory of Waves and Particles* (Springer, New York, 1982).
[2] W. H. Miller, J. Chem. Phys. **62**, 1899 (1975).
[3] W. H. Miller, S. D. Schwartz, and J. W. Tromp, J. Chem. Phys. **79**, 4889 (1983).
[4] T. Yamamoto, J. Chem. Phys. **33**, 281 (1960).
[5] R. Kubo, J. Phys. Soc. Jpn. **12**, 570 (1957).
[6] N. Moiseyev, J. Chem. Phys. **103**, 2970 (1995).

[7] W. H. Thompson and W. H. Miller, J. Chem. Phys. **102**, 7409 (1995); **106**, 142 (1997); H. Wang, W. H. Thompson, and W. H. Miller, *ibid.* **107**, 7409 (1997).
[8] U. Manthe, J. Chem. Phys. **102**, 9205 (1995); F. Matzkies and U. Manthe, *ibid.* **108**, 4828 (1998); **110**, 88 (1999).
[9] D. H. Zhang and J. C. Light, J. Chem. Phys. **106**, 551 (1997); D. H. Zhang, J. C. Light, and S.-Y. Lee, *ibid.* **109**, 79 (1998).
[10] T. Seideman and W. H. Miller, J. Chem. Phys. **96**, 4412 (1992).
[11] T. Seideman and W. H. Miller, J. Chem. Phys. **97**, 2499 (1992).
[12] U. Manthe and W. H. Miller, J. Chem. Phys. **99**, 3411 (1993).
[13] C. Leforestier and W. H. Miller, J. Chem. Phys. **100**, 733 (1994).
[14] S. M. Auerbach and W. H. Miller, J. Chem. Phys. **100**, 1103 (1994).
[15] A. Viel, C. Leforestier, and W. H. Miller, J. Chem. Phys. **108**, 3489 (1998).
[16] B. Poirier, J. Chem. Phys. **108**, 5216 (1998).
[17] U. Manthe, T. Seideman, and W. H. Miller, J. Chem. Phys. **99**, 10 078 (1993); **101**, 4759 (1994).
[18] W. H. Miller, in *Dynamics of Molecules and Chemical Reactions*, edited by R. E. Wyatt and J. Z. H. Zhang (Marcel Dekker, New York, 1996), p. 387; *Advances in Chemical Physics, Volume 101: Chemical Reactions and Their Control on the Femtosecond Time Scale*, XXth Solvay Conference on Chemistry, edited by P. Gaspard *et al.* (Wiley, New York, 1997), p. 853; *Photonic, Electronic and Atomic Collisions*, Proceedings of the XXth International Conference, edited by F. Aumayr and H. P. Winter (World Scientific, Singapore, 1998), p. 441.
[19] D. E. Manolopoulos and J. C. Light, Chem. Phys. Lett. **216**, 18 (1993).
[20] O. I. Tolstikhin, V. N. Ostrovsky, and H. Nakamura, Phys. Rev. Lett. **80**, 41 (1998). Equation (8) in this paper is given incorrectly: the order of the two matrix factors in the right hand side must be changed as in Eqs. (11) and (106) in this paper.
[21] S. Glasstone, K. J. Laidler, and H. Eyring, *The Theory of Rate Processes* (McGraw-Hill, New York, 1941).
[22] E. Gerjuoy, Ann. Phys. (N.Y.) **5**, 58 (1958).
[23] Yu. N. Demkov and V. N. Ostrovsky, Zh. Éksp. Teor. Fiz. **69**, 1582 (1975) [Sov. Phys. JETP **42**, 806 (1975)].
[24] V. N. Ostrovsky, J. Phys. B **24**, 4553 (1991); Phys. Rev. A **49**, 3740 (1994).
[25] P. P. Gorvat, V. Yu. Lazur, L. P. Presnyakov, and D. B. Uskov, Teor. Mat. Fiz. **91**, 66 (1992) [Theor. Math. Phys. **91**, 373 (1992)].
[26] E. P. Wigner and L. Eisenbud, Phys. Rev. **72**, 29 (1947).
[27] O. I. Tolstikhin, V. N. Ostrovsky, and H. Nakamura, Phys. Rev. Lett. **79**, 2026 (1997).
[28] O. I. Tolstikhin, V. N. Ostrovsky, and H. Nakamura, Phys. Rev. A **58**, 2077 (1998).
[29] *Atomic and Molecular Processes: An R-Matrix Approach*, edited by P. G. Burke and K. A. Berrington (IOP, Bristol, 1993).
[30] T. Seideman and W. H. Miller, J. Chem. Phys. **95**, 1768 (1991).
[31] C. Bloch, Nucl. Phys. **4**, 503 (1957).
[32] L. D. Faddeev and S. P. Merkuriev, *Quantum Scattering Theory for Several Particle Systems*, Mathematical Physics and Applied Mathematics, Vol. 11 (Kluwer Academic, Dordrecht, 1993).
[33] U. Fano, Phys. Rev. A **24**, 2402 (1981).
[34] J. Macek, J. Phys. B **1**, 831 (1968).
[35] See, e.g., appendix in A. T. Amos and G. G. Hall, Proc. Roy. Soc. **263**, 483 (1961).
[36] O. I. Tolstikhin and H. Nakamura, J. Chem. Phys. **108**, 8899 (1998).
[37] K. Nobusada, O. I. Tolstikhin, and H. Nakamura, J. Chem. Phys. **108**, 8922 (1998); J. Phys. Chem. **102**, 9445 (1998); J. Mol. Struct.: THEOCHEM **461-462**, 137 (1999).
[38] G. V. Mil'nikov, O. I. Tolstikhin, K. Nobusada, and H. Nakamura, Phys. Chem. Chem. Phys. **1**, 1159 (1999).
[39] O. I. Tolstikhin, S. Watanabe, and M. Matsuzawa, Phys. Rev. Lett. **74**, 3573 (1995).
[40] O. I. Tolstikhin, S. Watanabe, and M. Matsuzawa, J. Phys. B **29**, L389 (1996).
[41] K. L. Baluja, P. G. Burke, and L. A. Morgan, Comput. Phys. Commun. **27**, 299 (1982).
[42] A. Ohsaki and H. Nakamura, Phys. Rep. **187**, 1 (1990).
[43] A. Persky and M. Broida, J. Chem. Phys. **81**, 4352 (1984).
[44] H. Koizumi, G. C. Schatz, and M. Gordon, J. Chem. Phys. **95**, 6421 (1991).
[45] D. C. Chatfield, R. S. Friedman, S. L. Mielke, G. C. Lynch, T. C. Allison, D. G. Truhlar, and D. W. Schwenke, in *Dynamics of Molecules and Chemical Reactions*, edited by R. E. Wyatt and J. Z. H. Zhang (Marcel Dekker, New York, 1996), p. 323.
[46] M. Broida and A. Persky, Chem. Phys. **130**, 129 (1989).
[47] R. M. More and E. Gerjuoy, Phys. Rev. A **7**, 1288 (1973).
[48] A. J. F. Siegert, Phys. Rev. **56**, 750 (1939).
[49] V. Ryaboy and N. Moiseyev, J. Chem. Phys. **98**, 9618 (1993).
[50] O. I. Tolstikhin, I. Yu. Tolstikhina, and C. Namba, Phys. Rev. A **60**, 4673 (1999).